

A RADAR DESIGN FOR ATMOSPHERIC TURBULENCE STUDIES

by

Allan B. Plunkett

ANTENNAS AND PROPAGATION DIVISION
ELECTRICAL ENGINEERING RESEARCH LABORATORY
THE UNIVERSITY OF TEXAS
AUSTIN, TEXAS

GPO PRICE \$ _____

CFSTI PRICE(S) \$ _____

Hard copy (HC) 3.00

Microfiche (MF) 1.65

7 653 July 65

Report No. P-20

1 August 1967

N67-37465

FACILITY FORM 802

(ACCESSION NUMBER)

(THRU)

(PAGES)

(CODE)

(NASA CR OR TMX OR AD NUMBER)

(CATEGORY)

Prepared Under

NASA Grant NGR 44-012-048

3 A RADAR DESIGN FOR ATMOSPHERIC TURBULENCE STUDIES 6

by

6 Allan B. Plunkett 9

2 ANTENNAS AND PROPAGATION DIVISION 3
ELECTRICAL ENGINEERING RESEARCH LABORATORY
THE UNIVERSITY OF TEXAS
Austin, Texas 2

2AB
/ — END
Report No. P-20

9 1 August 1967 10 CV

Prepared Under

NASA Grant NGR 44-012-048 — 29A

1
25

ABSTRACT

Atmospheric turbulence can presently be measured only on the ground or by means of airplanes flying through the turbulent area. A properly designed radar system may be able to detect and analyze atmospheric turbulence from a position remote from the turbulent area. The choices of antenna, wavelength, transmitter power, receiver sensitivity, and detection methods are examined. The differences between pulse or cw and bistatic or monostatic systems are discussed. A comparison with existing radar systems used for atmospheric turbulence research is made.

TABLE OF CONTENTS

	Page
List of Figures	v
List of Tables	vii
I. Introduction	1
II. Radar Equation	4
III. Atmospheric Turbulence	6
IV. Antenna Considerations	17
V. System Wavelength Dependence	27
VI. Receiver	38
VII. Specific Systems	45
VIII. Conclustions	60
Bibliography	62

LIST OF FIGURES

Number		Page
1	Refractive Index Spatial Spectrum	7
2	Geometry	14
3	Normalized σ_v as a Function of Scattering Angle	14
4	Dependence of the Scattering Volume on the Pulse Length	16
5	Scattering Volume for Monostatic Radar	18
6	Scattering Volume for Bistatic Radar	20
7	Model for Calculating Scattering Volume	21
8	Parallelogram	21
9	Cross Section Parallel to yz Plane	22
10	Cross Section Parallel to the xz Plane	22
11	Relative Efficiency vs Wavelength for Backscatter Case	29
12	Relative System Efficiency for the Bistatic Radar	32
13	On Axis Power Density	34
14	Beam Spreading Factor	35
15	Dependence of the Minimum Range on Wavelength	36
16	Receiver Performance	42
17	Sky Temperature	43
18	Comparison of System Performance for Monostatic Radar	49
19	Integration Improvement Factor	51

20	Block Diagram of a Coherent Pulse Radar	52
21	Block Diagram of a cw Bistatic Radar	55

LIST OF TABLES

No.		Page
1	Monostatic Radar Parameters	48
2	Existing Systems	59

I. INTRODUCTION

The present study was instigated through a grant from the Electronics Research Center of the National Aeronautics and Space Administration for a study of clear air turbulence and methods for its detection. The present treatment includes detection methods of regions of disturbed refractive index in a broad sense and is not limited to clear air turbulence alone.

Radar return from the atmosphere is due to many factors including particulate matter such as rain, snow, sleet, bugs, birds, dust, etc., but, in addition, a radar signal may be scattered from regions of disturbed refractive index of the air. The scattering cross section of regions of disturbed refractive index is much less than the radar cross section of particulate matter such as rain.

The object of this study is to determine the radar system parameters necessary to detect and analyze radar returns from regions of disturbed refractive index, in particular, those related to clear air turbulence.

The major factors to be investigated are the system wavelength dependence, the difference between monostatic and bistatic radars, the desirability of using cw (continuous wave) or pulse radar and find the overall system performance required to detect and analyze turbulent regions.

A relatively simple model of the turbulent region will be used but the most critical features of size and degree of turbulence of the region will

be retained. An attempt will be made to state the assumed model clearly with references included to support the choice of model.

A. Nature of Clear Air Turbulence.

Clear air turbulence is defined as relatively severe turbulence of the atmosphere at high altitudes, usually above 20,000 feet. At lower altitudes, the atmosphere has a larger variation of refractive index due to the presence of water vapor. This greater variation produces a larger radar cross section for the low altitude case.

The scattering cross section of region of turbulent air will be evaluated both for backscatter and for scattering at other angles. In practice this is the weakest link in the chain of parameters involved in the detection system since our knowledge of the scattering cross section of the turbulent atmosphere is very limited. A few experimental results can be cited to obtain an estimate of the error involved in the application of the theory.

The radar equation is examined to determine the important factors in obtaining a usable return from the region of disturbed refractive index. These factors are then discussed individually.

The most important factor is the general structure of the turbulent region, which will determine the scattering cross section, and the size of the antenna.

Two difference types of emission are discussed, pulse and cw, and the methods of detection for each are examined.

B. Uncertainties in Refractive Index Structure and Suggestions for Clarification.

The characteristics of the variations in the index of refraction in the atmosphere are not completely understood, especially predictability. There have been several papers written on the possibility of detecting clear air turbulence by radar techniques. (2, 10, 17, 22) Some confirmation of turbulence theory, as applied to scattering of radio waves, is needed.

Variations in the dielectric constant of the air may or may not be easily related to the type of turbulence encountered by aircraft. Especially it would be desirable to discover what are the type of variations and the structure of these variations for the case of clear air turbulence. One way of more closely approaching this objective would be to make simultaneous radar measurements and refractive index measurements.

II. RADAR EQUATION

The relationship between the power transmitted and the power received is known as the radar equation^(3, 21). An examination of this equation will be necessary to determine which parameters can be optimized for detection of regions of disturbed refractive index of the atmosphere.

The radar equation is

$$P_R = \frac{G_T G_R \lambda^2 \sigma_v V P_T}{2(4\pi)^3 R_R^2 R_T^2} C_1$$

where

G_T = gain of transmitting antenna

G_R = gain of receiving antenna

λ = operating wavelength

σ_v = scattering cross section per unit volume

V = effective scattering volume

P_T = power transmitted

P_R = power received

R_R = range to receiver

R_T = range to transmitter

C_1 = beam filling factor.

The distribution of power across the beam is not uniform as assumed in the radar equation. A correction factor to reduce the power received

may be added to more nearly estimate the true received power. This factor is derived for a gaussian distribution of power across the beam by Probert-Jones⁽¹⁵⁾ and Stephens⁽²³⁾. This factor is $2 \ln 2 = 1.39$. In order to have a more conservative result and because the distribution is not gaussian, a factor of 2 is chosen. The various parameters in the radar equation are not independent of each other. For example, the antenna gain and beamwidth are related to wavelength. The scattering volume, which is defined by the pulse length and antenna beamwidth for the monostatic system or by the intersection of the two antenna patterns for the bistatic system, is dependent also on wavelength as well as other factors.

The size of the antenna beam defines the volume of turbulent air that will be illuminated. As the gain of the antenna increases, the effective scattering volume decreases. Hence, the optimum antenna size and gain need to be investigated with respect to changing wavelength. For best efficiency, the antenna beam should be filled, requiring that the extent of the turbulent region be estimated and the effective scattering volume shaped accordingly.

The standard radar parameters including transmitter power and modulation, receiver noise figure and detection systems, will be evaluated and conclusions drawn as to the optimum overall system for studying the atmosphere using radar.

III. ATMOSPHERIC TURBULENCE

Random variations of refractive index of the atmosphere occurring in a distance of the order of a wavelength will cause scattering of electromagnetic energy. This scattering is very small and thus a very sensitive radar system is necessary to detect it.

A. Turbulence Structure

The variations in refractive index with distance can be characterized as a random process with a space spectrum as shown in Figure 1. Tartarski⁽²⁵⁾ has shown that radar return is a function of the structure function defined by

$$D_n(r) = \overline{[N(o) - N(r)]^2}$$

where $N(o)$ and $N(r)$ are the refractive indices at two points separated by a distance r .⁽²¹⁾ When r is in the inertial subrange

$$D_n(r) = C_n^2 r^{2/3} \quad L_m \ll r \ll L_o$$

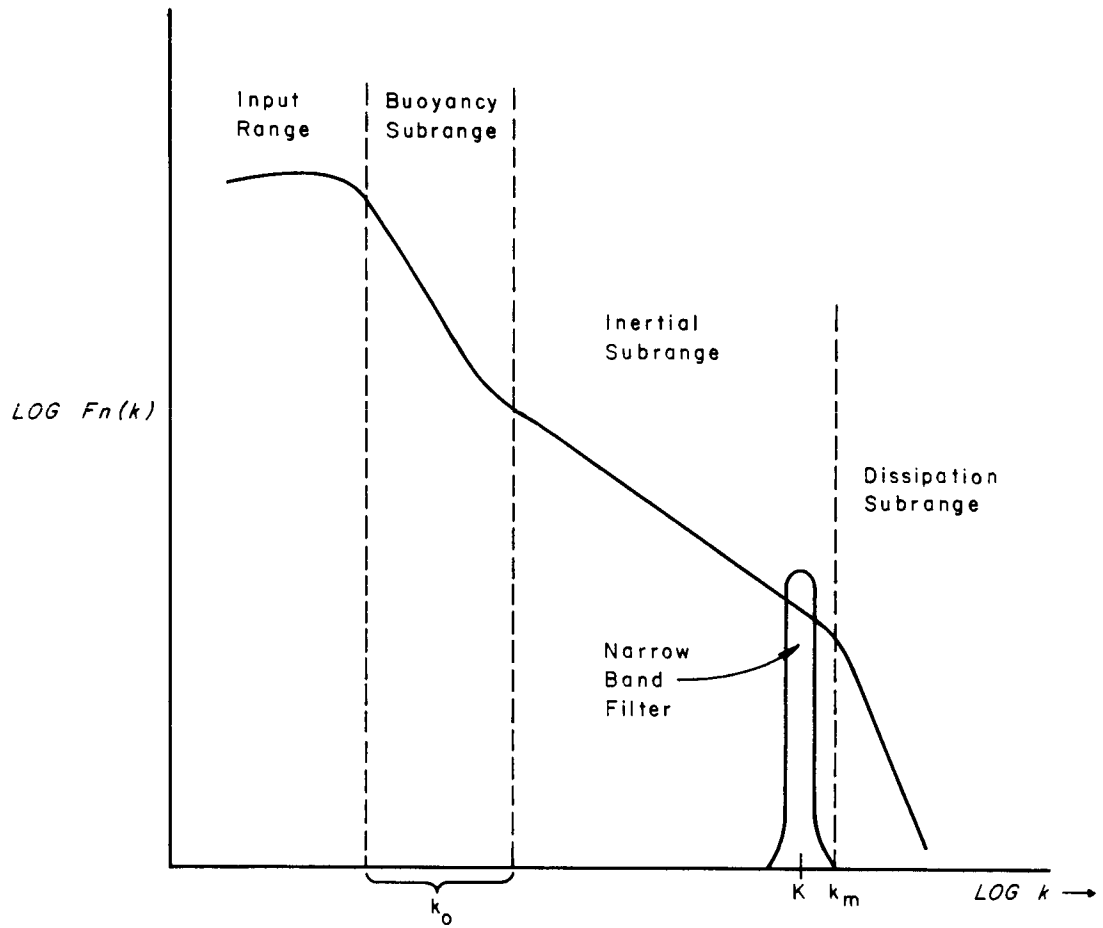
where C_n^2 is a constant depending on the strength of the turbulence. For r very large, the two samples $N(o)$ and $N(r)$ become independent and thus

$$\overline{[N(o) - N(r)]^2} = 2(\Delta n)^2.$$

Letting r equal L_o gives

$$(\Delta n)^2 \approx \frac{1}{2} C_n^2 L_o^{2/3}.$$

A more exact formula can be derived taking into account the fact that the $r^{2/3}$ variation does not extend to L_o . This formula is



NOTE: $K = \frac{4\pi}{\lambda} \sin \frac{\theta}{2} = \text{Selected Wave Number}$

Refractive Index Spatial
Spectrum

Figure 1

$$\overline{(\Delta n)^2} = .19 L_o^{2/3} C_n^2.$$

The one dimensional spatial spectrum that corresponds to this structure function is⁽²⁰⁾

$$F'_n(k) = .124 C_n^2 k^{-5/3}.$$

The Obukov spectrum is a normalized version of this. It is

$$F_n(k) = \frac{2}{3} k_o^{2/3} k^{-5/3}.$$

The radar return is controlled by the amplitude of the turbulence spectrum over a narrow range of the spacial wavelength centered at the radar's wavelength. This is represented in Figure 1 by the narrow band filter. Spectra have been measured over a limited range in the inertial subrange Austin, Texas using a set of four UHF (400 MHz) refractometers mounted in a three dimensional array. With spacings from 30 cm to 4 meters, the mean square value of difference in refractive index between temperatures was measured at a height above ground of about 75 meters and found to correspond to the spectrum in Figure 1. The data are, of course, nonstationary and contain large bursts probably caused by patches of higher water vapor content of the air at that instant. This would make the refractive index fluctuations much larger at low altitudes, enabling radar data to be obtained with a relatively simple system.

B. Clear Air Turbulence

Turbulence of the type that occurs in clear air lies in layers 500 to 3000 feet thick and up to 20 miles in horizontal extent. The system used to detect this turbulence must take this fact into account. An ordinary airborne radar may have only a very small percentage of its beam filled at a range sufficient to permit an aircraft time to take evasive action.

C. Problems in Detection

A jet plane must have at least one minute's warning in order to avoid turbulent areas. For a plane flying 600 mph, this requires a minimum detection range of ten miles. Some method of separation of the ground clutter from the air return must be employed. Without this separation, the radar window (area on the scope clear of ground clutter) for a pulse system is determined by the height of the plane which will be about six miles for the normal cruising altitudes of subsonic jet planes. Without the elimination of ground clutter, an adequate warning will not be available to the crew. Another problem with airborne radar is that of determining the height of a disturbance. At a range of ten miles, a five degree beamwidth (probably the minimum angle for the relatively long wavelength which appears to be better for turbulence detection) receives radar return from a height range of 5000 feet. This uncertainty in height gives the pilot little chance of avoiding the turbulence.

Thus, a ground-based research system seems to be the best possibility at present. Either a pulse monostatic or pulse or cw bistatic system could be used. A system of each type is described in this report.

As indicated earlier, clear air turbulence of the type that aircraft encounter seems to lie in layers 500 to 3000 feet thick and from 1 to 20 miles in horizontal extent^(8, 24). A vertically pointing radar would, therefore, have 100 per cent of its sampling volume filled with turbulence at some time as the turbulent area passes over. A ground-based bistatic system would also work well for the same reason.

D. Available Data

The general type of refractive index disturbance in the atmosphere up to 75 meters altitude has recently been measured in Austin, Texas with a three dimensional array of UHF refractometers. These measurements show that the turbulence spectrum is essentially the same as the theoretical one with values of about .25 N units occurring frequently. $N = (n - 1) 10^6$ where n is the index of refraction.

Average values of C_n^2 of $10^{-14} \text{ cm}^{-2/3}$ occur frequently. The structure of the turbulence appears to be mainly horizontal eddies. The size limit has not been reached with a refractometer spacing of 27 feet which was the maximum obtainable at the time. A reasonable assumption is that the eddies continually increase in intensity with size, with reasonably homogeneous turbulence at the smaller scales (one centimeter to one meter) of interest for radar measurements.

Structure function measurements indicate that the turbulent eddies are substantially horizontal with C_n^2 horizontally greater than C_n^2 vertically by about 25 per cent. Measured C_n^2 ranges from 10^{-13} to 10^{-15} with a five minute average of 10^{-14} at 80 meters height. At this altitude, water vapor has a strong effect on the radio refractive index of air and this factor undoubtedly causes the high values of C_n^2 that were measured. The variation of C_n^2 with altitude is essentially unknown.

Variations of refractive index with height have been measured. A ΔN of .2 may occur up to 16,000 feet altitude. The $\overline{\Delta N^2}$ variation with height is not constant but, in general, decreases with increasing height except for turbulent layers. (9)

The type of instruments used in obtaining this data is described in reference 18, the first section.

Stephens and Reiter⁽²⁴⁾ estimate the magnitude of C_n^2 for moderate turbulence. (20) Atlas, Hardy and Naito⁽²⁾ estimate C_n^2 to be $10^{-15} \text{ cm}^{-2/3}$ for moderate CAT and $10^{-14} \text{ cm}^{-2/3}$ for the most reflective CAT. (2) For the case under consideration, that is, a ground based radar observing relatively low altitude (up to 15,000 feet) turbulence, the magnitude of C_n^2 should be larger. Also, it is thought that water vapor may play a more significant part in the measurements made here which might account for the larger C_n^2 measured here ($10^{-13} > C_n^2 > 10^{-15}$). The purpose of correlating refractive index measurements with radar measurements to investigate

the general properties of atmospheric turbulence will be served by low altitude measurements and thus will not require as powerful a system as expected for Clear Air Turbulence.

Buehler and Lunden of the Boeing Company have had fair success with a VHF system (200 mHz) in detecting turbulence^(6, 7, 8, 12). They have installed a system in a Boeing 727 and flown it for 60 hours and have nine confirmed turbulence encounters of both radar sighting and airplane vibration at high altitude in clear air.

The radar volume scattering cross section for atmospheric turbulence has been derived from Tatarski's work by Atlas, et al⁽²⁾, and Stephens and Reiter⁽²⁴⁾ for random variations; for periodic variations by Smith and Rogers⁽²²⁾; and for a uniform gradient by Buehler and Lunden⁽⁶⁾.

E. Scattering Cross Section

The most useful scattering cross section in this case is the one based on Tatarski's theory. The general scattering cross section per unit volume is

$$\sigma = \frac{\pi \sin^2 \beta \overline{(\Delta n)^2} K^2 F_n(K)}{8 \sin^4 \frac{\theta}{2}}$$

where

θ = angle between the transmitter and receiver beams
(scattering angle)

β = angle between the direction of the receiver and the electric field of the transmitted wave

$\overline{\Delta n^2}$ = mean square refractive index value

$F_n(K)$ = one dimensional spectral density of $\overline{\Delta n^2}$

$$K = \frac{4\pi}{\lambda} \sin \frac{\theta}{2}$$

The Obukhov spectrum is $F_n(k) = \frac{2}{3} k_o^{2/3} k^{-5/3}$ where $k_o < k < k_m$.
 $k_o = \frac{2\pi}{L_o}$ and $k_m = \frac{2\pi}{L_m}$ where L_m and L_o are the inner and outer scales, respectively. L_m is approximately 1 cm for moderate turbulence and L_o is from 100 to 600 meters (2, 19).

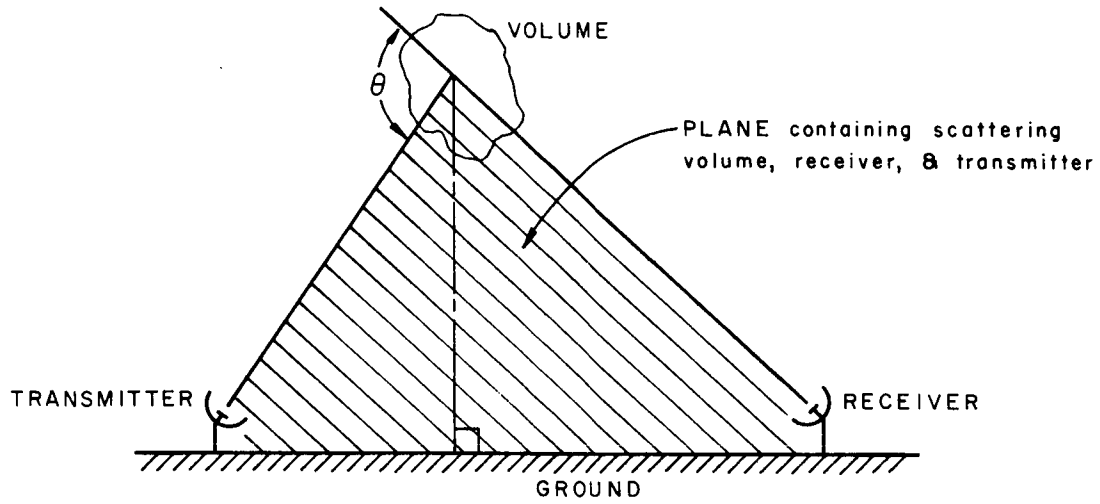
The $F_n(k)$ for the calculation of the scattering cross section is along the dotted line in Figure 2. The scattering cross section, in terms of C_n^2 , is derived below.

$$\sigma_v = \frac{\pi \sin^2 \beta \overline{(\Delta n)^2} K^2 F_n(K)}{8 \sin^4 \frac{\theta}{2}}$$

$$\sigma_v = \left(\frac{\pi \sin^2 \beta \overline{(\Delta n)^2} K^2}{8 \sin^4 \frac{\theta}{2}} \right) \left(\frac{2}{3} K_o^{2/3} K^{-5/3} \right)$$

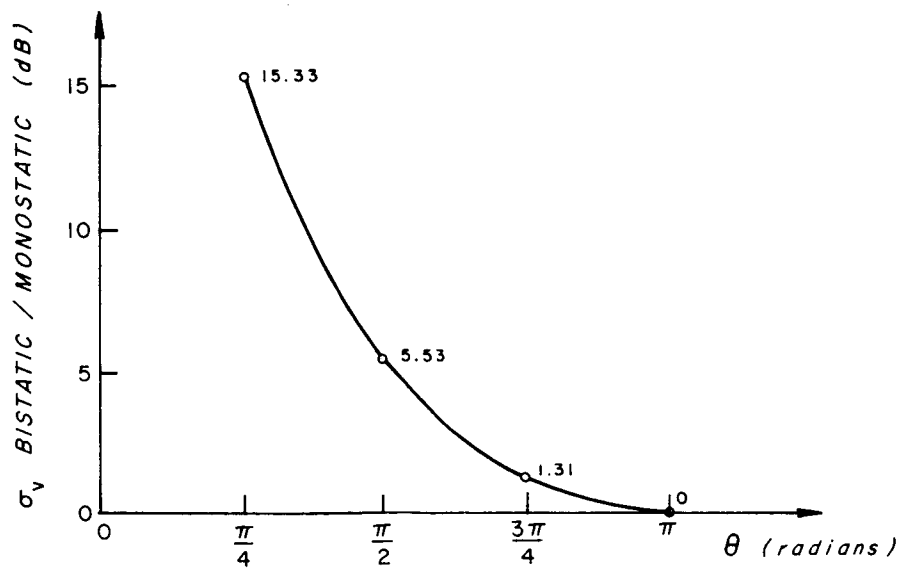
$$\overline{(\Delta n)^2} = 0.19 L_o^{2/3} C_n^2$$

$$\sigma = \frac{\pi}{12} [0.19 L_o^{2/3} C_n^2] \left[\frac{(2\pi)^{2/3}}{L_o^{2/3}} \right] \left[\frac{(4\pi)^{1/3}}{\lambda^{1/3}} \left(\sin \frac{\theta}{2} \right)^{1/3} \right] \frac{\sin^2 \beta}{\sin^4 \frac{\theta}{2}}$$



Geometry

Figure 2



Normalized σ_v as a Function
of Scattering Angle

Figure 3

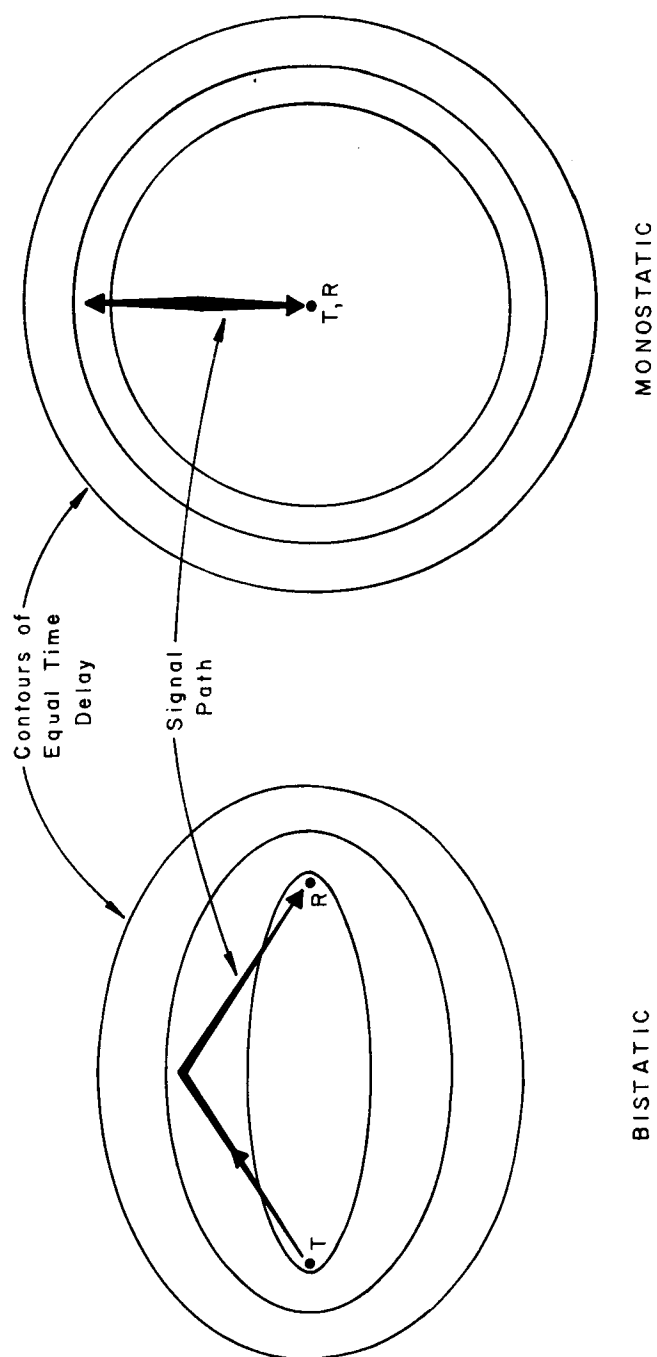
$$= .394 \sin^2 \beta \left(\sin \frac{\theta}{2} \right)^{-1/3} \lambda^{-1/3} C_n^2.$$

For backscatter ($\beta = \frac{\pi}{2}$, $\theta = \pi$)

$$\sigma_v = .394 \lambda^{-1/3} C_n^2.$$

The factor of $(\sin \theta)^{-1/3}$ in the bistatic case can give a large increase in cross section as the forward scattering condition is approached as shown in Figure 3.

The limits L_m and L_o permit the applicability of this cross section to wavelengths from about 1 cm to more than 100 meters. This covers most of the usable radar spectrum with scattering cross section peaking at $\lambda = 5 L_m$ or 5 cm. (2) The $\lambda^{-1/3}$ law is only accurate for $\lambda > 10 L_m$.



Note: For the monostatic case, the scattering volume is defined by $\frac{\tau}{2}$ due to the two way travel.

Dependence of the Scattering Volume
on the Pulse Length τ

Figure 4

IV. ANTENNA CONSIDERATIONS

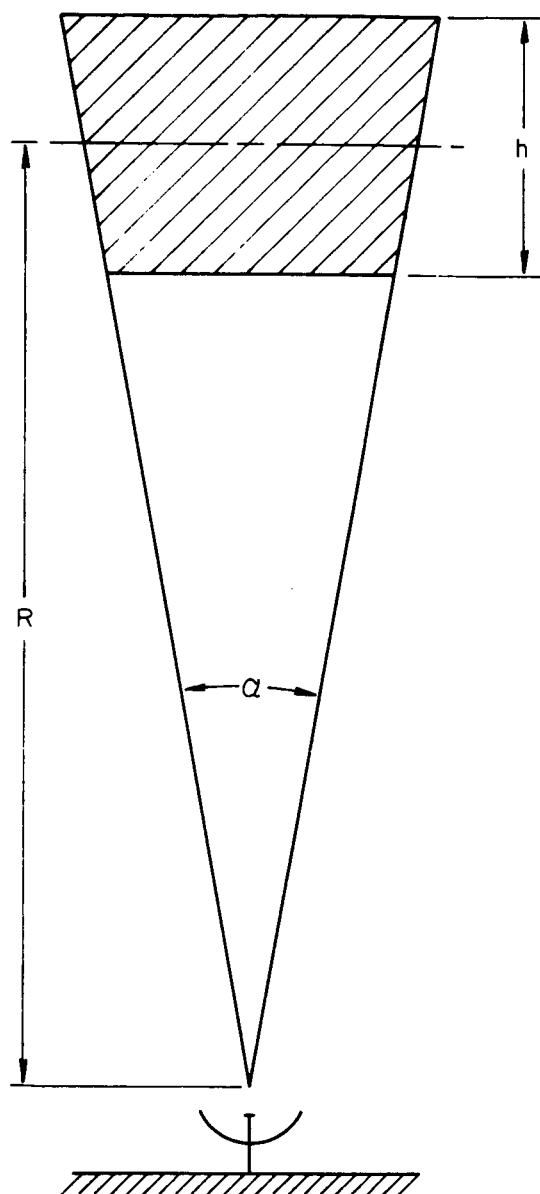
A. Volume for the Monostatic Case

The scattering volume will be calculated assuming the radiated power is concentrated within the 3 db points of the antenna beam. There is an additional effect which must be taken into account for backscatter of a pulse from a continuum of particles. At any instant after steady state, the power returned is due to the number of particles occupying the volume due to one half the pulse length (Figure 4).

This effect is due to the two way travel of the radar pulse. If the scattering angle θ is less than 90 degrees, the factor of one half can be removed.

The scattering volume must now be calculated (Figure 5).

$$\begin{aligned}
 V &= \int_0^{2\pi} \int_0^{\frac{\alpha}{2}} \int_{R-\frac{h}{2}}^{R+\frac{h}{2}} r^2 \sin \theta \, dr \, d\theta \, d\varphi = \int_0^{2\pi} \int_0^{\frac{\alpha}{2}} \left[\frac{r^3}{3} \right]_{R-\frac{h}{2}}^{R+\frac{h}{2}} \sin \theta \, d\theta \, d\varphi \\
 &= \frac{2\pi}{3} \left[\left(R+\frac{h}{2}\right)^3 - \left(R-\frac{h}{2}\right)^3 \right] \left[1 - \cos \frac{\alpha}{2} \right] \\
 &= \frac{2\pi}{3} \left[\frac{h^3}{4} + 3R^2h \right] \left[1 - \cos \frac{\alpha}{2} \right] = \frac{2\pi}{3} \left[\frac{h^3}{4} + 3R^2h \right] \left[1 - \left(1 - \frac{\alpha^2}{2} + \frac{\alpha^4}{4} \dots \right) \right] \\
 &= \frac{\pi}{3} \left[\frac{h^3}{4} + 3R^2h \right] \alpha^2. \\
 \alpha &= .612 \frac{\lambda}{a} \text{ radians where } a \text{ is the diameter of the aperture.} \quad (26)
 \end{aligned}$$



$\alpha = 3$ db beamwidth

$$h = \frac{c\tau}{2}$$

$R =$ range

$\tau =$ pulse length

$$c = 3 \times 10^8 \frac{\text{m}}{\text{s}}$$

Scattering Volume for
Monostatic Radar

Figure 5

With this substitution,

$$V = .392 \left[\frac{h^3}{4} + 3R^2h \right] \left(\frac{\lambda}{a} \right)^3 .$$

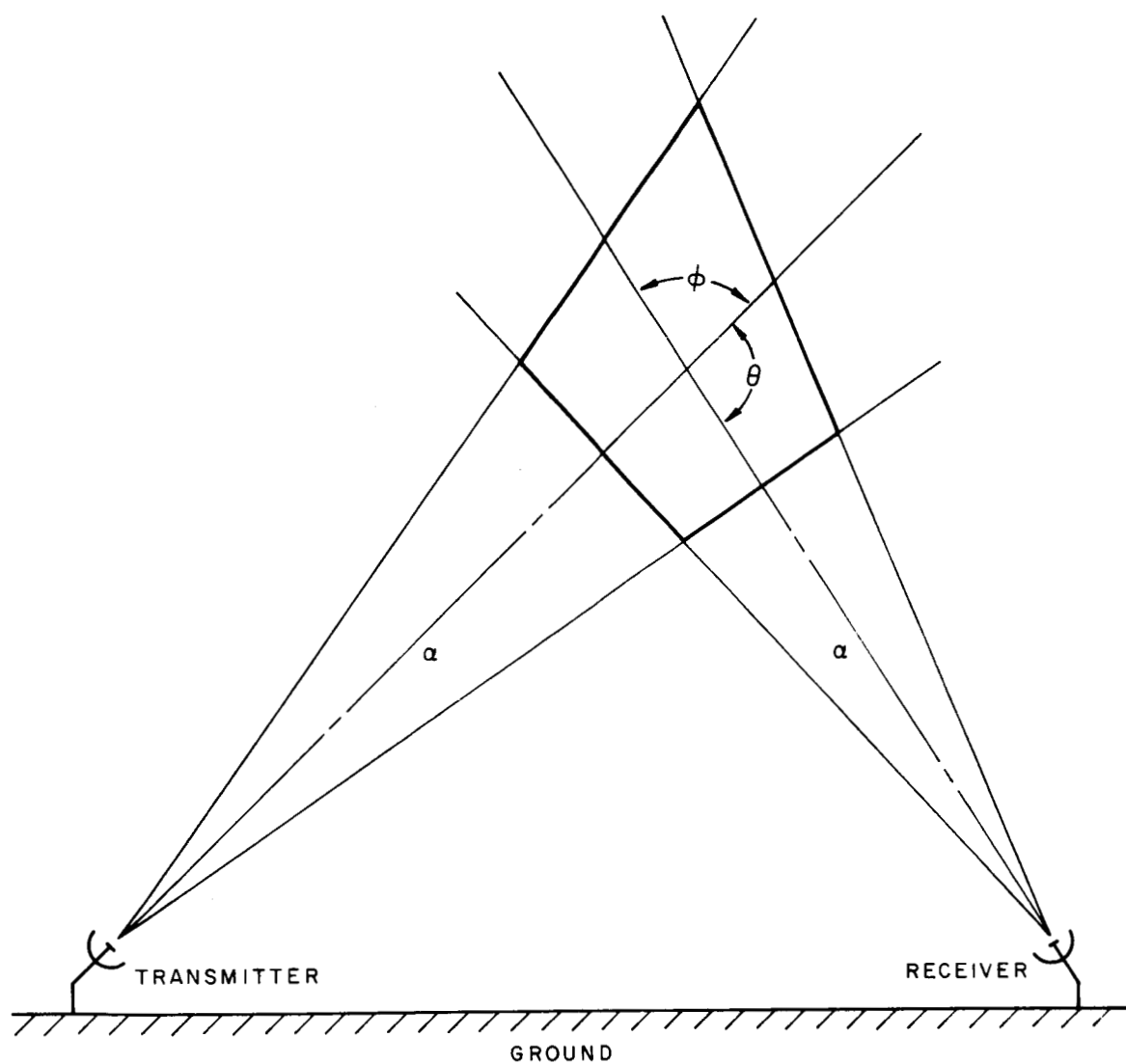
The pulse length will be chosen to optimize the returned signal from a horizontal layer 500 to 3000 feet thick. Therefore, for a 1000 foot thick layer (a median value), a pulse length of $2\mu s$ will be optimum as $h = \frac{c\tau}{2}$.

B. Volume for Bistatic Case

For the bistatic radar case, the scattering volume will be assumed to be defined entirely by the intersection of the antenna beams. The scattering volume geometry is illustrated in Figure 6. The problem of calculating the volume can be much simplified if the beams are assumed cylindrical. This assumption will hold when the length of the intersection is less than $\frac{1}{10}$ of the range to the volume. The two intersecting cylinders are shown in Figure 7.

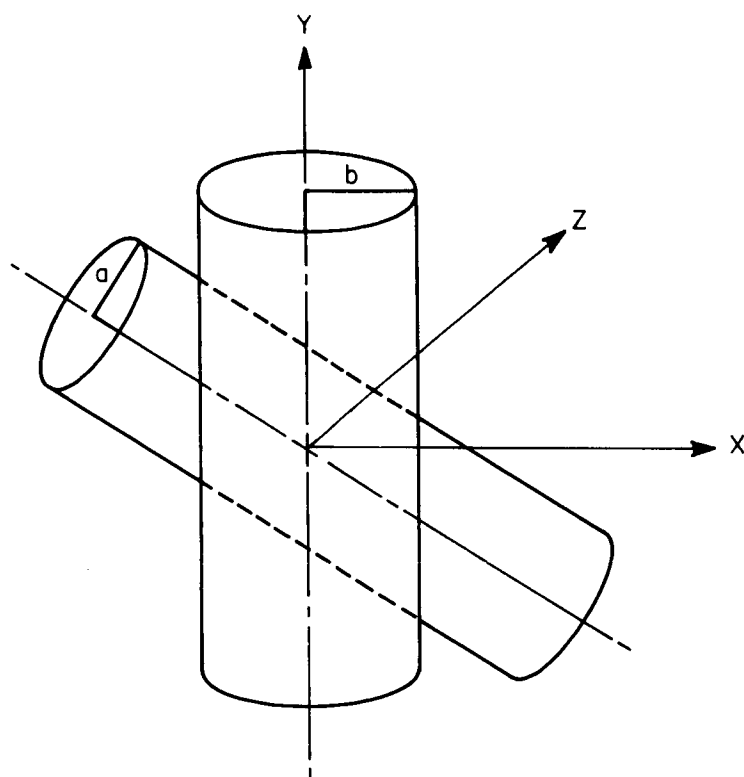
The scattering volume may be thought of as a stack of parallelogram shaped slices of dz thickness. The sum of all these slices equals the total volume.

To calculate the common volume, take slices of the intersection parallel to the xy plane (Figure 8). Next, take a cross section parallel to the yz plane to get the variation in c and d which are the edges of the parallelogram (Figure 9).



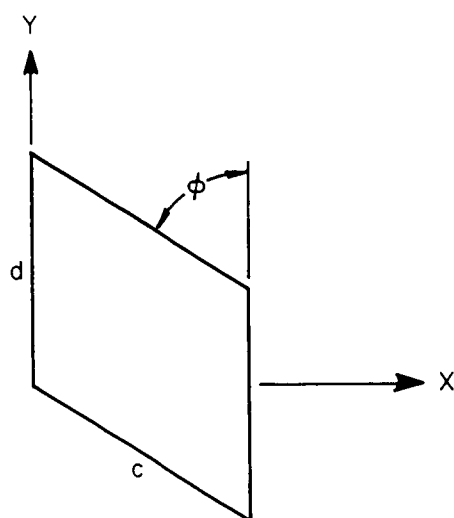
Scattering Volume for Bistatic Radar

Figure 6



Model for Calculating Scattering Volume
for Bistatic Radar

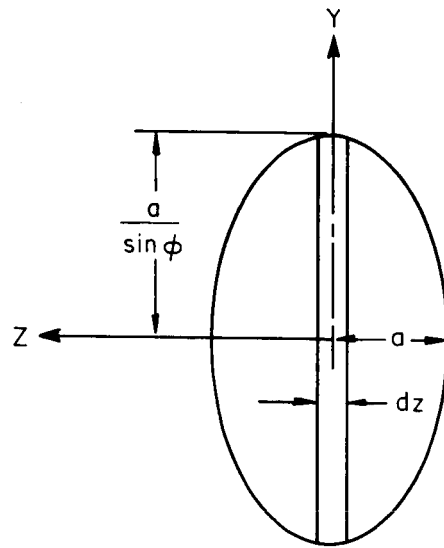
Figure 7



Note: Area of parallelogram = $cd \sin \varphi$

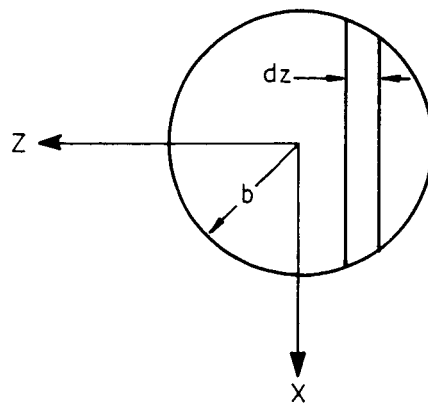
Parallelogram

Figure 8



Cross Section Parallel to yz Plane

Figure 9



Cross Section Parallel to the xz Plane

Figure 10

$$\frac{z^2}{a^2} + \frac{y^2}{a^2} \sin^2 = 1$$

is the equation of this ellipse (Figure 8). From this

$$y = \frac{\sqrt{a^2 - z^2}}{\sin \phi}.$$

Now take cross-section parallel to the xz plane (Figure 10). The equation of this circle is

$$x^2 + z^2 = b^2.$$

From this

$$x = \sqrt{b^2 - z^2}.$$

Sum up the volumes of all the parallelograms of depth dz, dimensions

$$d = \frac{2\sqrt{a^2 - z^2}}{\sin \phi} \quad \text{and} \quad c = \frac{2\sqrt{b^2 - z^2}}{\sin \phi}$$

$$V = 2 \int_0^d \frac{4\sqrt{a^2 - z^2} \sqrt{b^2 - z^2}}{\sin^2 \phi} \sin \phi \, dz \quad \text{where } d = \min \{a, b\}.$$

For the case when $a = b$

$$V = \frac{8}{\sin \phi} \int_0^a (a^2 - z^2) \, dz = \frac{16 a^3}{3 \sin \phi}$$

Since $\varphi = 180^\circ - \theta$, $\sin \varphi = \sin \theta$ and the volume becomes

$$V = \frac{16a^3}{3 \sin \theta}.$$

But $a = R \frac{\alpha}{2}$

where α is the antenna beam angle and R is the range to the center of the volume. So the volume is

$$V = \frac{16}{3} \frac{(R \frac{\alpha}{2})^3}{\sin \theta} = \frac{2}{3} \frac{R^3 \alpha^3}{\sin \theta} = .153 \frac{R^3}{\sin \theta} \left(\frac{\lambda}{a} \right)^3$$

in terms of parameters already defined and used in the radar equation.

C. Limitations on Antenna Size

The size of the antenna determines both the gain and the scattering volume, so that the choice of antenna size is not immediately obvious.

Another factor of importance is the change in the antenna characteristics at close range due to the transition from the Fraunhofer to Fresnel regions.

This gives a minimum range limitation which is

$$R = \frac{D^2}{\lambda}$$

R = range

D = diameter

λ = wavelength.

For this criterion, the true gain is .94 of the Fraunhofer gain which is a small loss for this application⁽²⁰⁾. Page 28 gives a more complete analysis of this situation.

$$\lambda = \sqrt{\frac{7A}{G}} = \sqrt{\frac{7(\pi r^2)}{G}} = r\sqrt{\frac{7\pi}{G}}$$

$$= (750) \left(\frac{7\pi}{10^5} \right)^{1/2} = 11.1 \text{ cm}$$

At wavelengths longer than 11 cm, a constant antenna size of 15 meters will be assumed and at wavelengths shorter than 11 cm, a constant gain of 50 db will be assumed for the maximum antenna size and gain.

V. SYSTEM WAVELENGTH DEPENDENCE

The system effectiveness as a function of wavelength can now be found.

The radar equation is

$$P_R = \frac{G_T P_T G_R \lambda^2 \sigma_v V}{2(4\pi)^3 R_R^2 R_T^2} C_1$$

where P_T , R_R , R_T will be assumed constant with respect to wavelength for this calculation. The scattering cross-section is

$$\sigma_v = .394 (\sin \beta)^2 \left(\sin \frac{\theta}{2}\right)^{-11/3} \lambda^{-1/3} C_N^2.$$

σ_v has a $\lambda^{-1/3}$ wavelength dependence for wavelengths greater than about 10 cm but σ_v does not obey the $\lambda^{-1/3}$ law for shorter wavelengths. For wavelengths between 10 cm and 3 cm σ_v will be approximately constant. (2)

A. Backscatter Case

First, the radar equation for the single antenna, pulse radar will be written. For a $1\mu s$ pulse length, the volume becomes

$$V = 35 \left(\frac{\lambda}{a}\right)^2 [7.5 \times 10^3 + R^2] \text{ meters}^3$$

for $R \gg a$

where a = diameter of antenna.

For wavelengths shorter than 11 cm, G_T , G_R and σ_v will be constant, so

$$\begin{aligned}
P_R &= \lambda^2 \frac{V}{2} \left(\frac{P_T G_T G_R \sigma_v C_1}{2(4\pi)^3 R_R^2 R_T^2} \right) \\
&= \lambda^2 \left[353 \left(\frac{\lambda}{a} \right)^2 (7.5 \times 10^3 + R^2) \right] \left(\frac{P_T G_T G_R \sigma_v C_1}{2(4\pi)^3 R_R^2 R_T^2} \right) \\
&= (\text{constant}) \lambda^4.
\end{aligned}$$

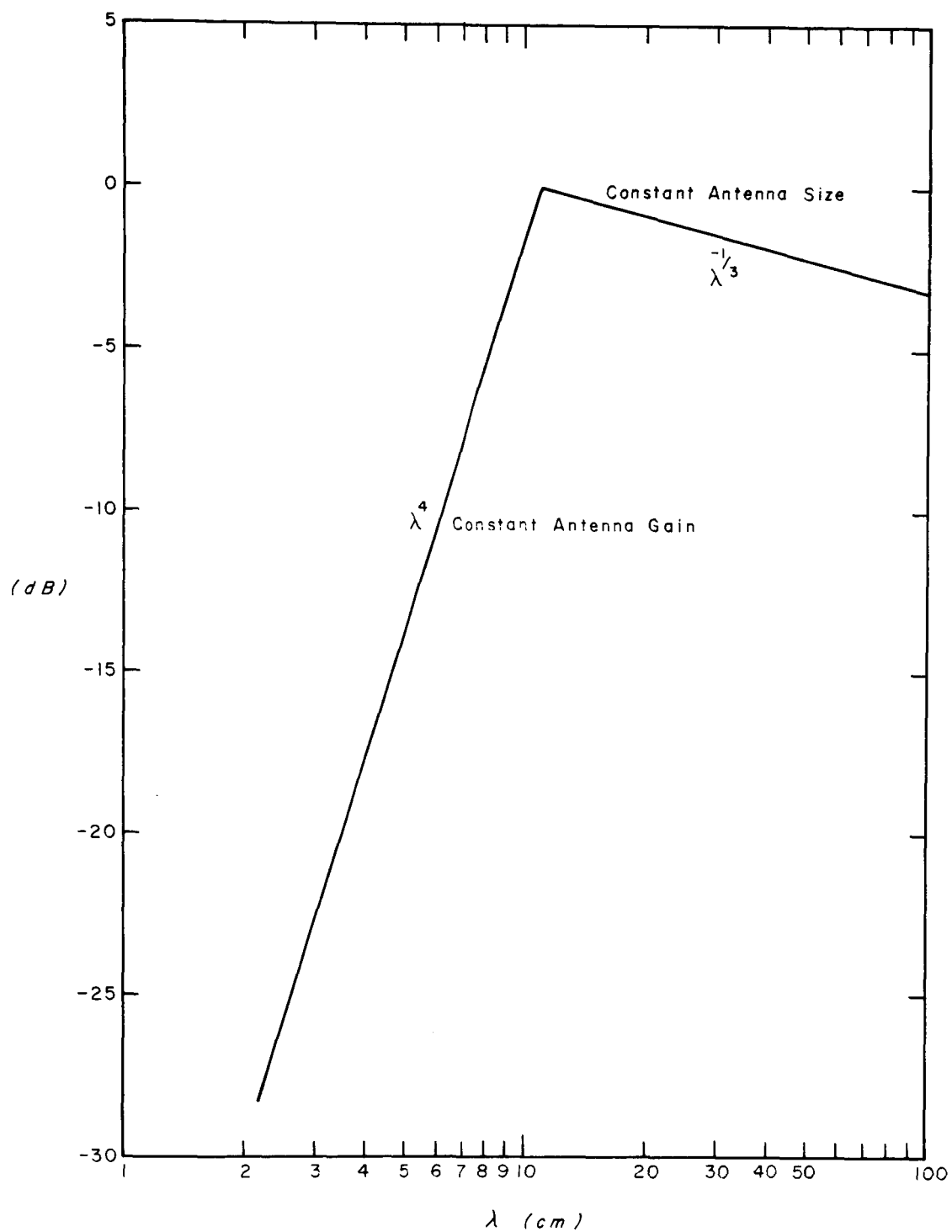
This equation shows that for wavelengths shorter than 11 cm, there is a severe penalty in received signal to noise ratio for the assumed system as the wavelength decreases.

However, for wavelengths greater than 11 cm, the situation is quite different. The gain is no longer constant and neither is σ_v . The gain is

$$G = \frac{7A}{\lambda^2} = \frac{7\pi a^2}{\lambda^2}.$$

The received power now becomes

$$\begin{aligned}
P_R &= \left(\frac{P_T C_1}{2(4\pi)^3 R_R^2 R_T^2} \right) \\
&\times \left[\frac{7\pi a^2}{\lambda^2} \right] [\lambda^2] [.394 \lambda^{-1/3} C_n^2] \left[353 \left(\frac{\lambda}{a} \right)^2 (7.5 \times 10^3 + R^2) \right] \\
&= (\text{constant}) \lambda^{-1/3}.
\end{aligned}$$



Relative System Efficiency for the Monostatic Radar

Figure 11

The received signal strength is now substantially independent of frequency with a slight penalty for longer wavelengths. Over a wavelength range of 10 cm to 1 meter there will be a reduction in signal-to-noise ratio of only about 3 db which is fairly small. However, good receiver noise figure and high transmitted power are more easily obtained with less cost at the longer wavelengths.

In order to have a small sample size to get some idea of the statistics of the turbulence and to have a symmetrical volume, the wavelengths between 10 cm and 30 cm would probably be the best. Figure 11 shows a plot of the relative efficiency of the system against wavelength for the backscatter case.

At the longer wavelengths and long ranges, the volume may become so large as to not be completely filled causing a drop in the efficiency greater than that shown. If the curve for constant antenna size were extended for $\lambda < 11$ cm, it would level off due to the change in the dependence of σ_v on wavelength.

B. Bistatic Case

For the bistatic radar, the wavelength dependence will be different due to the fact that the volume is proportional to the third power of the beam width instead of the second power.

For scattering angles (θ) less than about 120 degrees, the radar wavelength will appear to be lengthened. The radar samples the magnitude

of the structure function $F_n(K)$ at a wavenumber $K = \frac{4\pi}{\lambda} \sin\left(\frac{\theta}{2}\right)$ (see Figure 1); therefore, as the scattering angle θ becomes less, the wavenumber K becomes less. The effect of this is to cause the $\lambda^{-1/3}$ law for the scattering cross section to apply for shorter radar wavelengths.

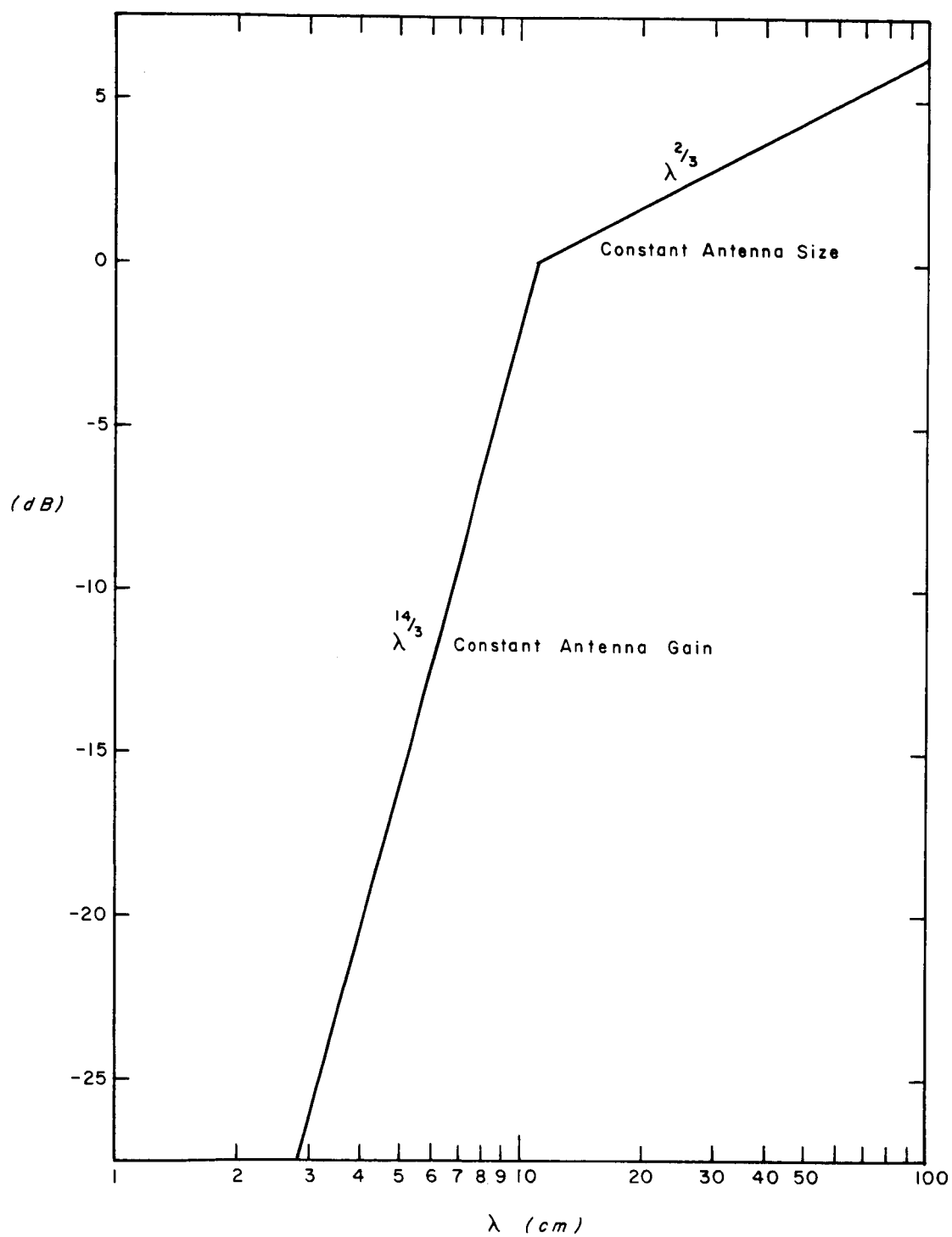
The wavelength dependent for the bistatic case will be found using the same criteria for the antennas of a constant gain of 50 db for $\lambda < 11$ cm and a constant diameter of 15 meters for $\lambda > 11$ cm.

For the short wavelength case, the radar equation becomes

$$\begin{aligned}
 P_R &= \frac{P_T G_T G_R C_1 \lambda^2 V \sigma_v}{2(4\pi)^3 R_R^2 R_T^2} \\
 &= (\text{constant}) (\lambda^2) \left(.153 \frac{R^3}{\sin \theta} \left(\frac{\lambda}{a} \right)^3 \right) \left(.394 \sin^2 \beta \sin^{-11/3} \frac{\theta}{2} \lambda^{-1/3} C_n^2 \right) \\
 &= (\text{constant}) \lambda^2 \lambda^3 \lambda^{-1/3} = (\text{constant}) \lambda^{14/3}, \quad \lambda < 11 \text{ cm.}
 \end{aligned}$$

For the long wavelength case

$$\begin{aligned}
 P_R &= \frac{P_T G_T G_R C_1 \lambda^2 V \sigma_v}{2(4\pi)^3 R_R^2 R_T^2} \\
 &= (\text{constant}) G_T G_R \lambda^2 V \sigma_v \\
 &= (\text{constant}) \left(\frac{7\pi a^2}{\lambda^2} \right) (\lambda^2) \left(.153 \frac{R^3}{\sin \theta} \left(\frac{\lambda}{a} \right)^3 \right) \left(.394 \sin^2 \beta \sin^{-11/3} \frac{\theta}{2} \lambda^{-1/3} C_n^2 \right) \\
 &= (\text{constant}) \lambda^{2/3}.
 \end{aligned}$$



Relative System Efficiency for the Bistatic Radar

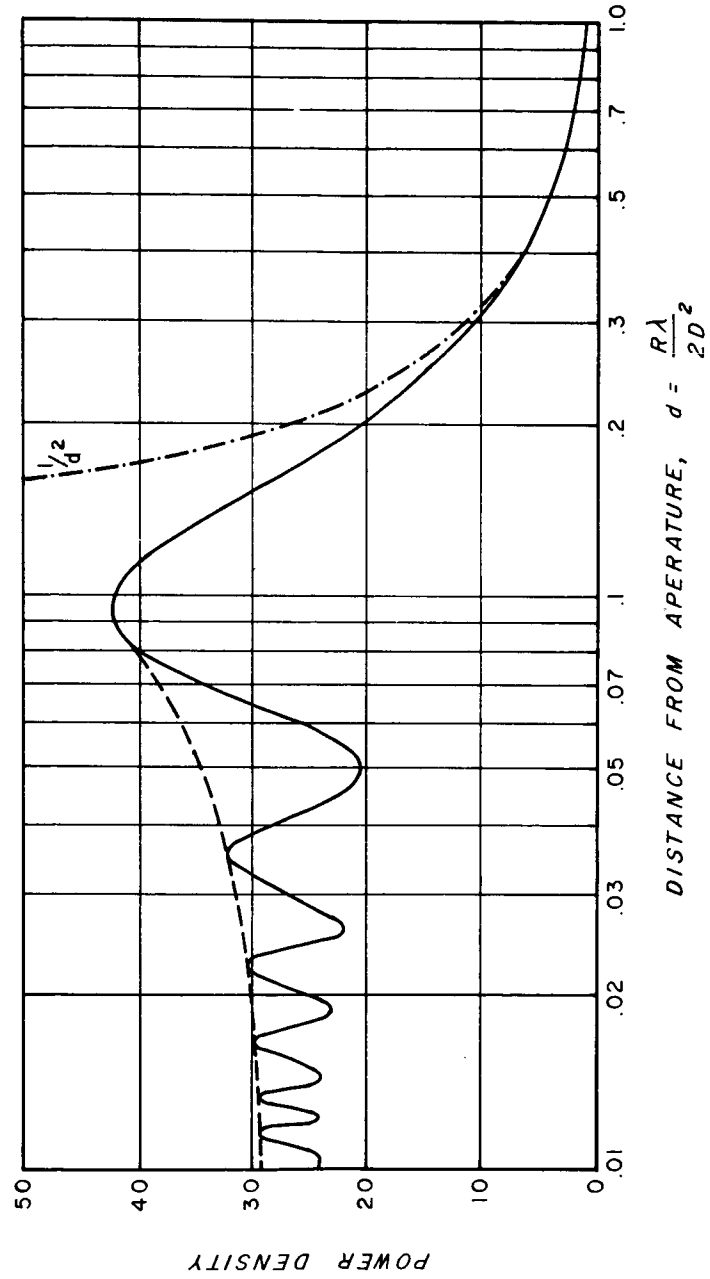
Figure 12

The reason for the greater dependence on wavelength for the bistatic case is that the volume is defined completely by the beamwidth whereas in the monostatic case the pulse length defines one dimension. These results are plotted in Figure 12 for comparison with the backscatter case. Notice that the curve for $\lambda > 11$ cm rises instead of drops.

For low altitudes (less than one or two kilometers) disturbed refractive index, the scattering volume will be small enough that it will be fairly well filled and these system efficiencies will be realized.

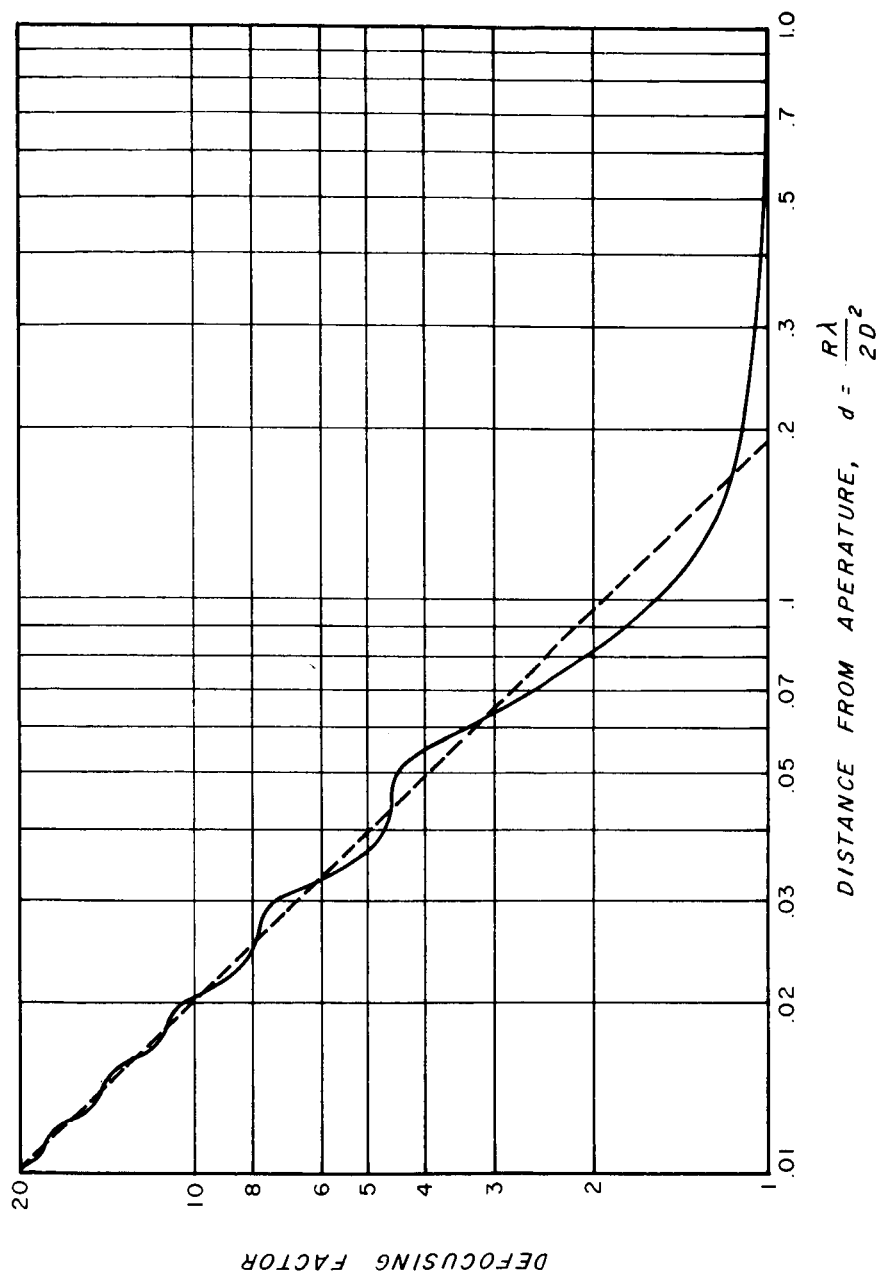
There will be a minimum range for which radar studies can be carried out. This is due to being within the Fresnel region of the antenna for which the basic assumptions of the radar equation are invalid. For both the bistatic and backscatter radars, the range will be that from the scattering volume to the antenna but the bistatic system will be able to look at lower altitudes and still measure the $F_n(K)$ vertically (see Figure 2).

The boundary between the Fraunhofer and Fresnel regions is actually a gradual change from one to the other. By using $R = \frac{D^2}{\lambda}$ as mentioned before, the predictions of scattering volume and gain of the antennas will still be fairly close to the true values. From Figures 13 and 14 the peak radiated power density occurs at $R = .2 \frac{D^2}{\lambda}$. The beamwidth at this range is approximately twice that in the far field. ⁽⁵⁾ A plot of the minimum operating range vs. wavelength is given in Figure 15 for the previous assumptions; that is, for $\lambda < 11$ cm, a constant antenna gain of



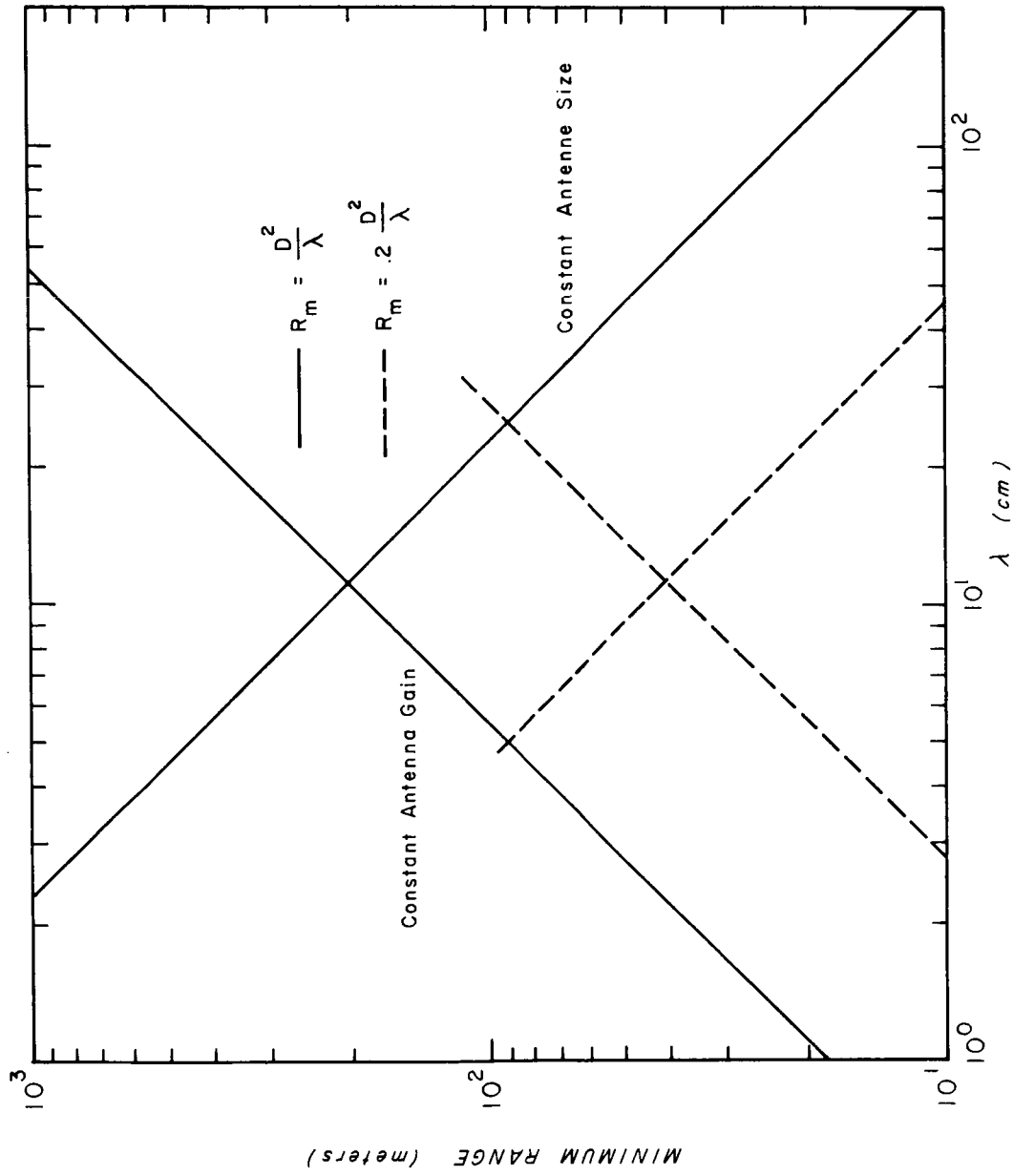
On Axis Power Density for a Circular Aperture
with Tapered Illumination

Figure 13



Defocusing Factor for a Circular Aperture
with Tapered Illumination

Figure 14



Dependence of the Minimum Range on Wavelength

Figure 15

50 db is assumed and for $\lambda > 11$ cm, a constant antenna size of 15 meters is assumed.

For accuracy in gain and beamwidth calculations, the minimum range $\frac{D^2}{\lambda}$ should be used; however, the minimum range at which usable gain is obtained is at $R = \frac{.2D^2}{\lambda}$ but inaccuracies in the antenna surface and phase error across the aperture make the gain and beamwidth calculations only approximate.

For low altitude observations with a 50' antenna, the best wavelength would be about 30 cm giving a minimum range of about 750 meters. At low altitudes, it would be possible to measure with refractometers the disturbed refractive index at the same time as the radar measurements are taken. The antenna size would have to be reduced below 15 meters for shorter wavelengths in order to stay within the far field when the backscatter system is used.

VI. RECEIVER

A very sensitive receiver will need to be employed in order to achieve the maximum signal-to-noise ratio on the radar return. The ordinary crystal mixer front end is far too noisy unless extremely high transmitter power is used. This consideration dictates the use of some sort of low noise amplifier before the mixer. There are several types available; among these are tunnel diode amplifiers, parametric amplifiers using varactor diodes, masers using ruby crystals, traveling wave tubes, and transistor amplifiers.

A. Signal-to-Noise Ratio

The noise level at the input to the receiver limits the usable receiver sensitivity. This noise comes from several sources for microwave radar. The most important of these is the noise introduced by the receiver itself. For example, the equivalent noise temperature of the sky at microwave frequencies is approximately 50°K, but the receiver noise temperature for a crystal mixer (usual type) will be about 2500 to 5000°K.

The equivalent noise temperature is defined as the temperature of a resistor at the input of a noiseless receiver (matched to the input impedance of the receiver) that produces the same noise power output as from the noisy receiver. The relationship used is

$$N = K_b T_e B$$

where

N = noise power

$K_b = 1.38 \times 10^{-23}$ (Boltzman's constant)

B = integrated noise bandwidth

T_e = effective noise temperature in °K.

The noise power output is independent of the resistance which makes the power relation more useful than the voltage one since

$$V_N^2 = 4K_b T_e B R$$

and the receiver input impedance must be known. The bandwidth is the integrated noise bandwidth which is

$$B = \int_{-\infty}^{\infty} H(f) df \approx 3\text{db bandwidth.}$$

A more useful measure of the effectiveness of the system than the received power alone is the received signal-to-noise ratio.

$$\frac{S}{N} \text{ received} = \frac{P_R}{N}$$

where

N = noise power introduced in the system.

Now,

$$\frac{S}{N} = \frac{P_R}{N} = \frac{P_R}{K_b T_e B} \text{ (assuming white noise).}$$

T_e is defined the following way:

$$T_e = T_{\text{sky}} + T_{\text{ref}} \left[(F_1 - 1) + \frac{(F_2 - 1)}{G_1} + \frac{(F_3 - 1)}{G_1 G_2} + \dots + \frac{(F_i - 1)}{G_1 G_2 \dots G_{i-1}} + \dots \right] \text{ } ^\circ\text{K}$$

where the noise figure F_i is the signal-to-noise ratio at the output of stage i divided by the input signal-to-noise ratio, G_i is the gain of stage i and $T_{\text{ref}} = 290^\circ\text{K}$. The radar equation now becomes

$$\frac{S}{N} = \frac{P_T G_T G_R \lambda^2 \sigma_v V C_1}{2(4\pi)^3 R_R^2 R_T^2 K_b T_e B}$$

B. R. F. Amplifiers

All of these types of R. F. (radio frequency, i. e., before the mixer) amplifiers are not suitable for this application.

The maser amplifier is very expensive and requires a complicated cooling unit. For this application, all of the leakage power cannot be eliminated. The maser saturates with a power level greater than about -35 dbm which is not too difficult to obtain. However, it recovers very slowly (1 ms) which makes it almost impossible to use for a pulse system. These objections, along with the cost, make the maser a poor choice for this purpose.

Traveling wave tubes are expensive and do not exhibit better noise figures than parametric amplifiers and tunnel diodes. Therefore, these would probably not be as useful.

For microwave frequencies ($\lambda < 30$ cm), this leaves the parametric amplifiers and tunnel diode amplifiers. Both of these have fast recovery time ($< 1\mu\text{s}$) and both have high saturation levels⁽⁴⁾.

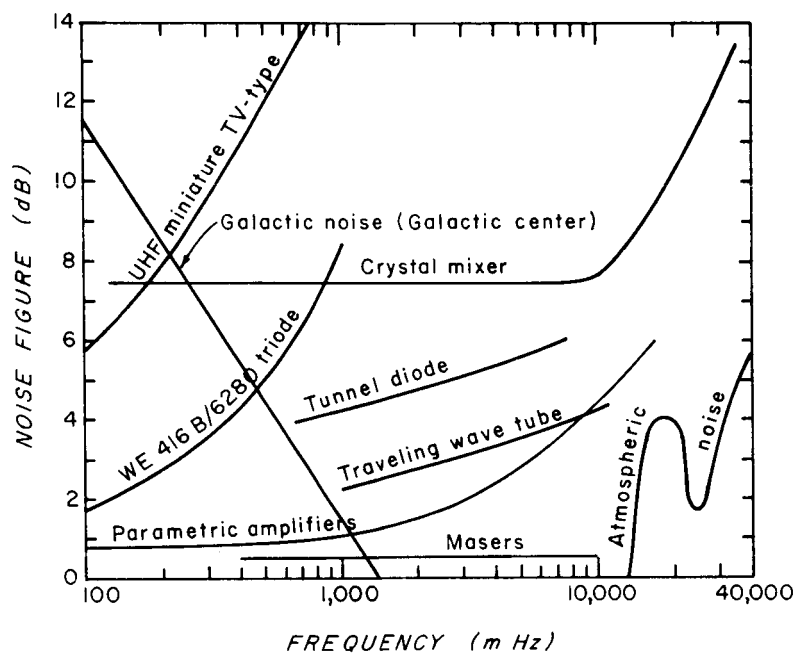
Parametric amplifiers can have noise figures of about 2 db while a noise figure of 4.5 db is typical for a tunnel diode amplifier. Either amplifier will be suitable for use in a turbulence detection system.

At wavelengths about 1 meter, a greater variety of amplifiers is available. Transistor amplifiers can be built for low cost with noise figures of 2 db for frequencies of 400 MHz and below. Thus, greater receiver sensitivity with less cost is possible at VHF frequencies. A plot showing the relative noise figures of various receivers as a function of frequency is given in Figure 16.^(4, 21)

C. External Noise

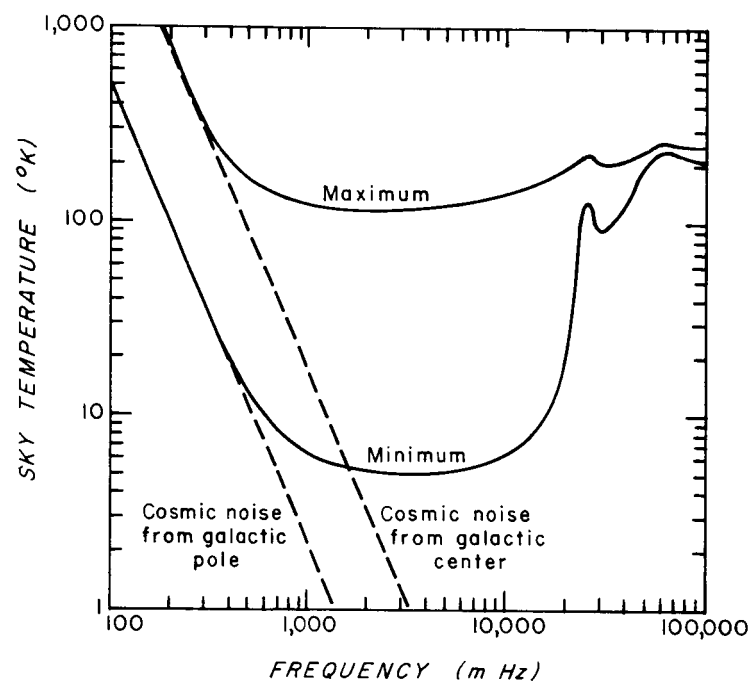
Another factor limiting the effective noise temperature in this frequency range is radio noise from extraterrestrial objects and the earth's atmosphere. This noise is a function of frequency and the pointing direction of the antenna. Noise from extraterrestrial objects can be minimized by pointing away from the galactic center, sun, and moon. The atmospheric noise is minimum when the antenna is pointing vertically and is maximum for horizontal pointing.

The maximum and minimum sky temperature as seen by an ideal antenna are given in Figure 17.⁽²¹⁾ The maximum and minimum curves



Receiver Performance

Figure 16



Sky Temperature

Figure 17

for galactic noise occur when the antenna is pointed at the galactic center and the galactic pole. The maximum and minimum curves for atmospheric noise are for horizontal pointing and vertical pointing.

The atmospheric and galactic noise set the minimum usable noise figure of the receiver to about 10 to 50 degrees K.

VII. SPECIFIC SYSTEMS

Two types of radar systems for research on disturbed refractive index in the atmosphere are to be designed. The first type is a monostatic pulse radar with a vertically pointing antenna. The second is a bistatic radar with the two antennas widely enough separated to give a scattering angle between 90 and 160 degrees. The system parameters are estimated for $\lambda = 3, 10, 30$, and 100 cm.

A. Monostatic (backscatter) Radar

1. Radar Equation

The radar equation for this case becomes

$$\frac{S}{N} = \frac{G^2 \lambda^2 P T_v^\sigma}{128 \pi^3 R^4 K_b T_e B} \times \frac{VC}{2}$$

where

$\frac{S}{N}$ = signal-to-noise ratio at the receiver output

R = range

G = antenna gain

$\sigma_v = 394 \lambda^{-1/3} C_n^2$, C_n^2 ranges from $10^{-14} \text{ cm}^{-2/3}$ at low altitudes to $10^{-16} \text{ cm}^{-2/3}$ or less at higher altitudes

$K_b = 1.38 \times 10^{-23} \text{ joule/}^\circ\text{K}$

B = receiver bandwidth

h = pulse length

P_T = power transmitted

λ = wavelength

C = beam filling factor

$V = .392 \left(\frac{h^3}{4} + 3R^2h \right) \left(\frac{\lambda}{a} \right)^2$ = scattering volume

2. System Parameters

The pulse length is chosen as $2\mu s$ (600 meters in space) so that the scattering volume is approximately as long as a turbulence layer is thick. The minimum receiver bandwidth is 1 MHz due to the pulse length of $2\mu s$. The beam filling factor will be approximately unity for most clear air turbulence as it lies in horizontal layers about 300 meters thick and up to 10 km in extent. The receiver RF amplifier has an assumed noise figure of 4 db for $\lambda = 3$ and 10 cm, 3 db for $\lambda = 30$ cm, and 2 db for $\lambda = 100$ cm. The gain is assumed to be 15 db. Either tunnel diode or parametric amplifiers can meet these specifications. The amplifiers for $\lambda = 30$ or 100 cm could be a transistor amplifier which would be less expensive than the parametric amplifier. The receiver mixer is chosen as a crystal mixer with a noise figure of 9 db. The IF amplifier has a 1 mc bandwidth with a noise figure of 2 db. Losses in the transmission line and duplexer will be assumed to be $\frac{1}{2}$ db. The antenna noise temperature is assumed to be 60°K. This noise is due to the sky temperature plus noise entering via the side lobes⁽²¹⁾. The

system parameters are listed in Table 1. Figure 18 shows the single pulse received signal-to-noise ratio as a function of range for the four frequencies.

Figure 18 shows that the performance of the 3 cm system is much less than that of the longer wavelength systems. This is largely due to the reduction of the effective area of the antenna for receiving. Figure 18 also shows that at these short ranges, only a moderate peak power of 10^5 watts would be necessary for a reasonable signal-to-noise ratio in order to analyze the type of disturbance causing the return. It is desirable to limit the sample size in order to be able to tell more about the structure of the turbulence which would be best accomplished with either the 10 cm or 30 cm systems. As far as cost is concerned, the 100 cm system would be the optimum.

3. Detection Methods

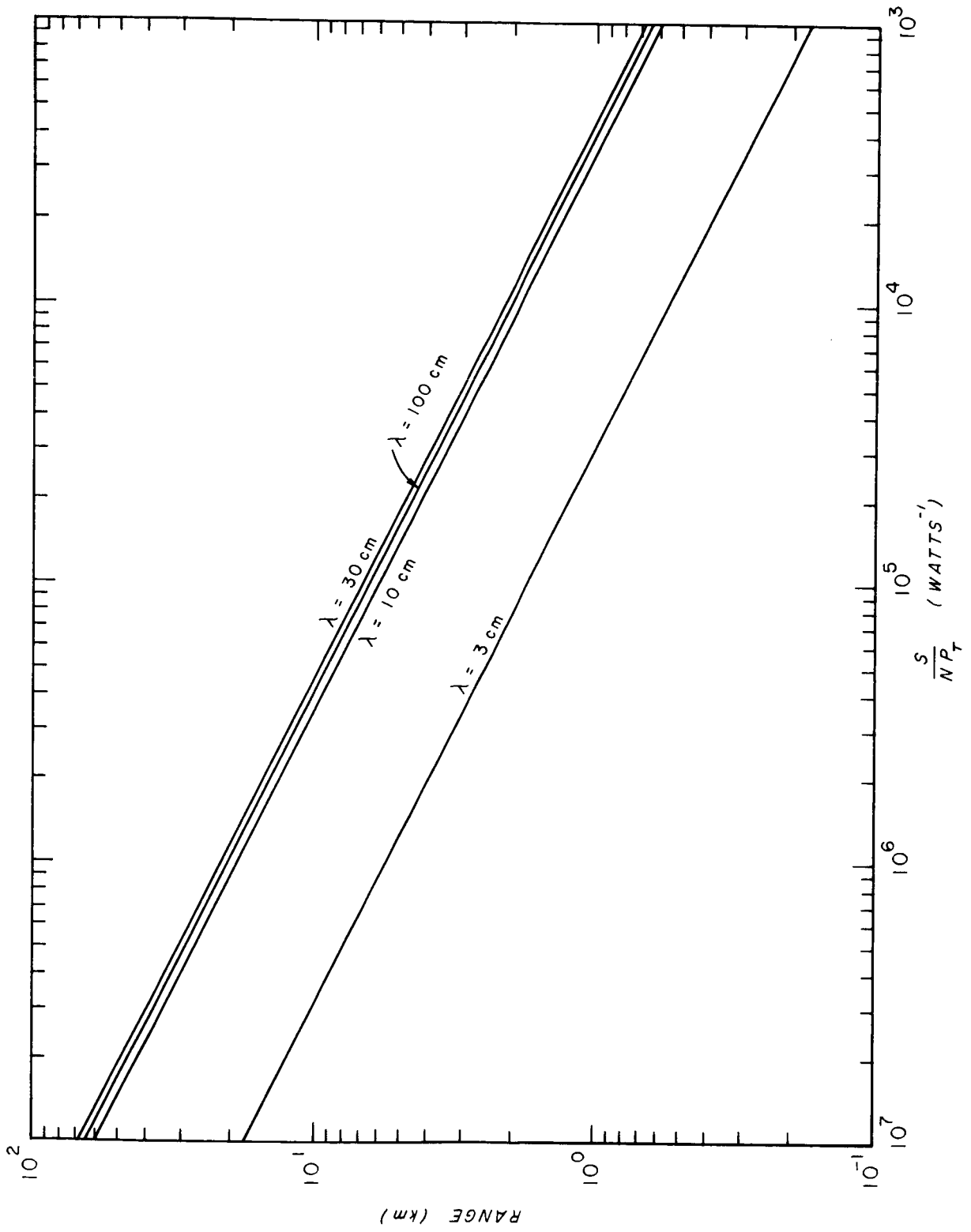
The method of detection can change the effective signal-to-noise ratio of the received signal from that predicted by the single pulse signal-to-noise ratio to which the radar equation as used so far applies.

The maximum rate of change of the signal scattered from a turbulent region will be about 50 Hz to 100 Hz. This means that each pulse will not be independent of the preceding pulse if the prf (pulse repetition frequency) is greater than 200 Hz. For this application, a prf up to 10,000 Hz can be used. A simple system to take advantage of this redundancy in the received pulse train is to integrate the received

Table 1

Monostatic Radar Parameters

	λ			
	3 cm	10 cm	30 cm	100 cm
size, dia.	4.05 m	13.5 m	15 m	15 m
Antenna gain	50 db	50 db	41.4 db	31 db
beamwidth	.519°	.519°	1.4°	4.66°
Scattering volume	$\frac{3.86 \times 10^{-2}}{R^2}$	$\frac{3.86 \times 10^{-2}}{R^2}$	$\frac{.282}{R^2}$	$\frac{3.14}{R^2}$
$R \geq 10^3$ m				
σ_v for $C_n^2 = 10^{-16} \text{ cm}^{-2/3}$	1.83×10^{-15}	1.83×10^{-15}	1.27×10^{-15}	$.85 \times 10^{-15}$
RF amp. NF	4 db	4 db	3 db	2 db
gain	15 db	15 db	15 db	15 db
crystal mixer plus NF	9 db	9 db	9 db	9 db
I.F. amp.				
Loss before R.F. amplifier	.5 db	.5 db	.5 db	.5 db
T_e	760°K	760°K	500°K	355°K
T_e crystal mixer receiver only (no RF amp)	2350°K	2350°K	2350°K	2350°K
Max. Range for detection of $C_n^2 = 10^{-16} \text{ cm}^{-2/3}$ with $P_T = 10^6$ watts (single pulse $\frac{S}{N} = 1$)	5.5 Km	18.5 Km	21.2 Km	20.8 Km



Comparison of System Performance for Monostatic Radar

Figure 18

signal with a low pass filter after the detector. For a 10 kHz prf and a 100 Hz low pass filter, the number of pulses integrated is $\frac{10,000}{100} = 100$. The noise is uncorrelated from one pulse to the next and thus does not add in the integrator as the signal does. If the signal is detected in an envelope detector, the phase information is lost and the integration efficiency is much less than expected. Figure 19 shows the relationship between the number of pulses integrated and the integration improvement factor defined as

$$\frac{S}{N} \text{ (after integration)} = I \frac{S}{N} \text{ (single pulse)}^{(21)}.$$

For a multiplier type detector as used with a coherent radar,

$$I = n$$

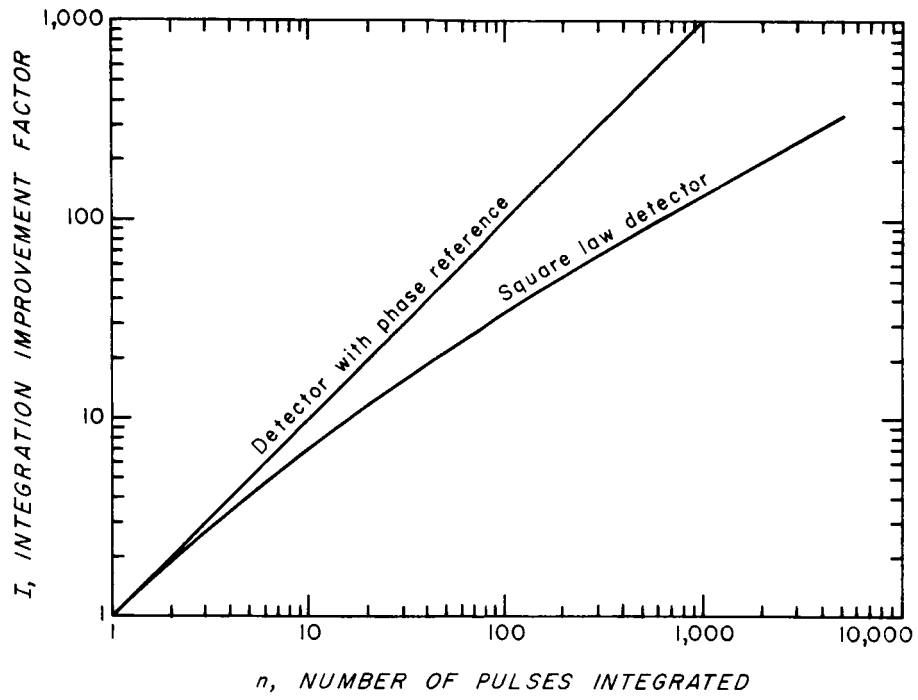
where n = number of pulses integrated.

In the example above the 100 pulses integrated,

$$\text{effective } \frac{S}{N} = 35 \frac{S}{N} \text{ (single pulse)}$$

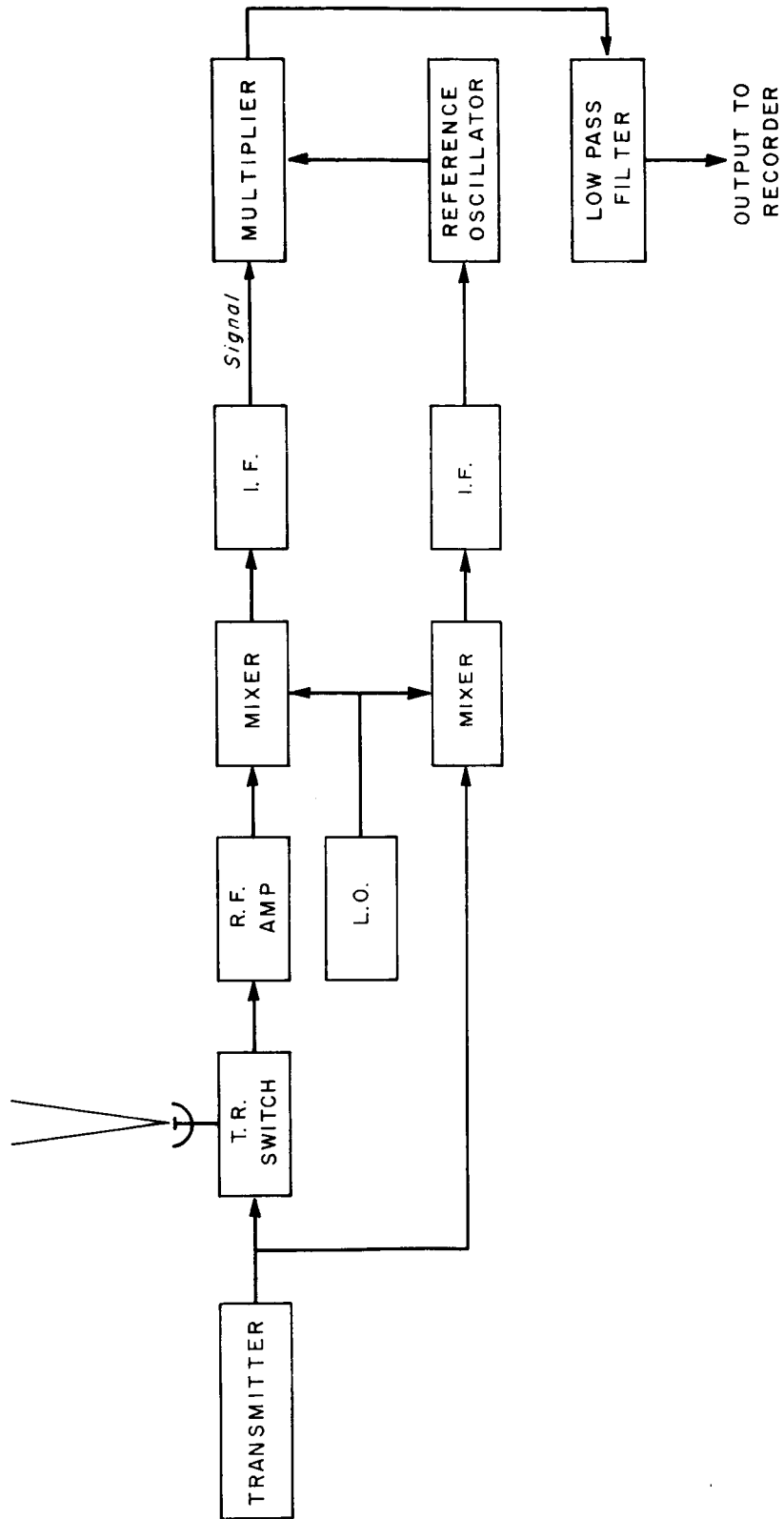
when an envelope detector is used.

The transmitted pulse may be used to phase synchronize an oscillator which will then supply a reference signal of the proper phase to a multiplier type detector. The result will be that the phase information will be retained and the integration improvement factor will be equal to the number of pulses integrated, or 100 for the example. This may be done as shown in the block diagram in Figure 20.



Integration Improvement Factor

Figure 19



Block Diagram of a Coherent Pulse Radar

Figure 20

B. Bistatic Radar

The bistatic radar performance when using a pulse system is substantially the same as the vertically pointing backscatter system except for the increase in σ_v due to the reduced scattering angle. This increase will be about 5 db for a 90° scattering angle. However, the bistatic radar allows the scattering volume to be defined entirely by the intersection of the beams of the two antennas thus allowing CW operation.

CW operation of a radar for the 100 cm wavelength for a transmitter power of about 1000 watts is relatively easy to obtain for low cost compared with a microwave system of the same power. Using this coherent transmitter, the receiver can use a reference from the transmitter to mix with the received signal from the disturbed region. A multiplier type detector would probably be the best to use as it has a linear characteristic. By this means both the amplitude spectrum and doppler of the turbulent air can be measured and knowledge of the speed of the moving air can be obtained.

Moderate turbulence has a gust velocity of 20 to 30 mph or 9 to 13 meters/sec. For vertical motion, the doppler frequency shift is given by

$$fd = \frac{2V}{C}$$

V = vertical velocity of target

C = phase velocity.

Therefore, the doppler frequency for the 100 cm radar will vary between 18 to 26 Hz. This means that a very small receiver bandwidth of about 50 Hz can be used.

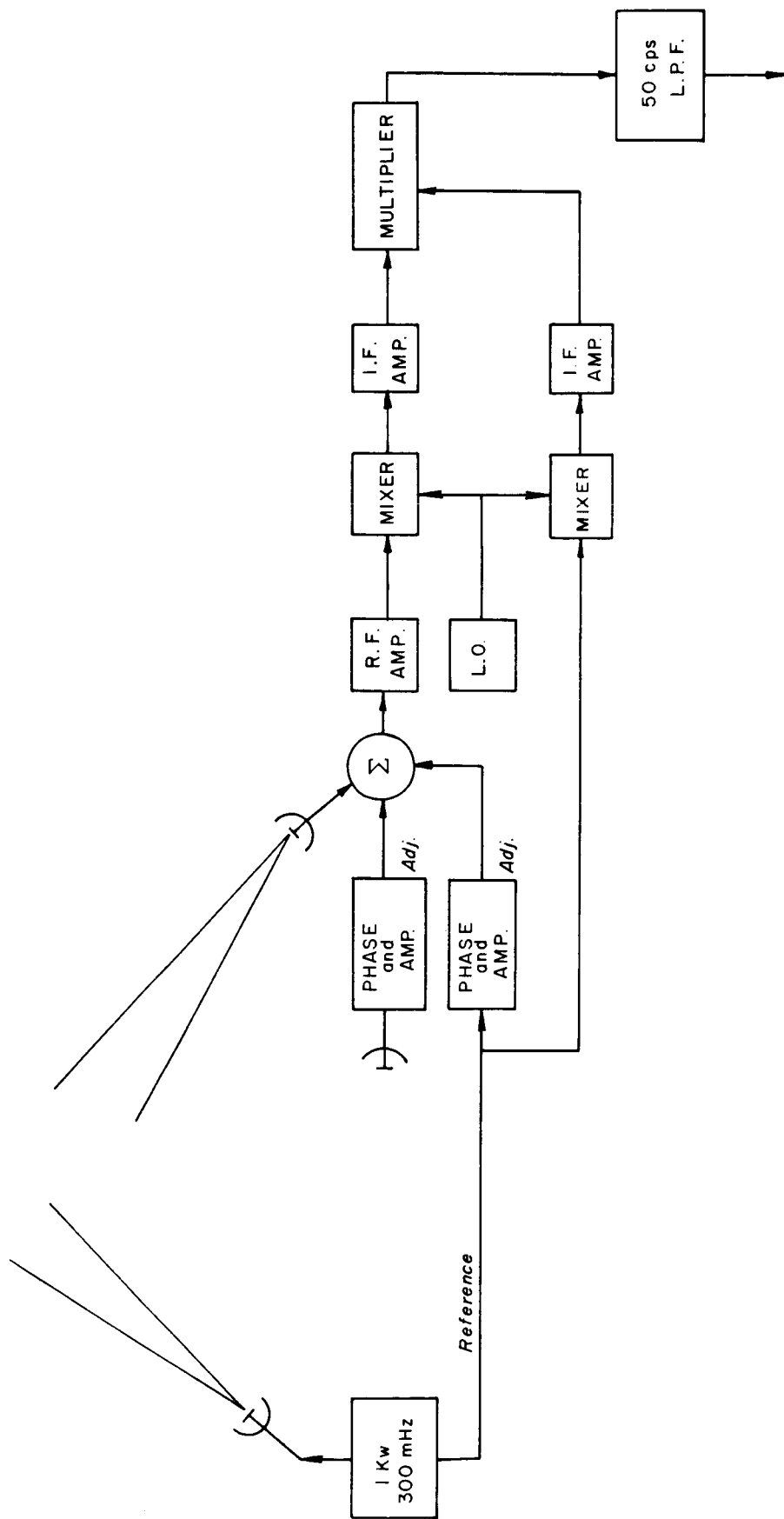
By putting a 50 cps filter at the output of a linear detector, the effect of a 100 cps I. F. bandwidth can be obtained. Figure 21 illustrates the system for this case.

With a coherent system of this type, two methods of clutter reduction are possible. The transmitter signal can be directly carried to the receiver by a coax cable and then adjusted in amplitude and phase to cancel the clutter; also, a separate antenna can be used to pick up the transmitter signal directly and this signal added to the signal from the main antenna to cancel the clutter.

To obtain a comparison with the monostatic system, a representative maximum range calculation is made using the same parameters as before except for $P_t = 1$ Kw and receiver bandwidth = 100 Hz. The antennas are assumed to be 2 Km apart, elevated 45° to give $\theta = 90^\circ$ and use horizontal polarization to give $\beta = 90^\circ$.

	backscatter		bistatic CW
	single pulse	coherent detector	
$\frac{S}{N} / P_t$	4.3×10^{-4}	.086	.872

For a 10 db signal-to-noise ratio, the transmitted power would have to be about 25 Kw (pulse) for backscatter or 11.5 watts for the bistatic



Block Diagram of cw Bistatic Radar

Figure 21

system (CW). The average power of the coherent pulse radar for a prf of 10 kHz and pulse length of $2\mu\text{s}$ would be 23 watts or twice that of the CW radar. This is due to the smaller scattering volume for the backscatter pulse radar. A precedent for this low power is the system used at Boeing using a 74 MHz, 100 watt CW transmitter and a receiver bandwidth of about 50 Hz. Signals from disturbed refractive index at altitudes of 20,000 to 30,000 feet of up to 10 db over the noise level.

The main disadvantage is that separate antennas are required; however, this probably would be necessary for the backscatter radar in order to achieve the low noise and clutter levels required.

C. Comparison with Other Systems

Other researchers have detected radar echoes which are due to some type of disturbed refractive index of the atmosphere. Among these are Saxton, et al.⁽¹⁷⁾; Atlas, Hardy and Glover⁽¹⁾; and Buehler and Lunden^(6,7,8,14). Atlas, et al, have detected turbulence associated with a tropopause at about 10 to 12 Km. The measured radar cross section was about $7.7 \times 10^{-17} \text{ cm}^{-1}$ corresponding to $C_n^2 = 4.4 \times 10^{-16} \text{ cm}^{-2/3}$. Saxton, using a much less powerful radar, detected refractive index variations due to turbulence in layers at altitudes of 2 to 3 Km. These observations by Saxton were not measured quantitatively.

Buehler and Lunden at a site in Seattle, Washington, have seen many times, with a VHF radar, echoes which are apparently associated

with turbulence. These echoes have been observed up to about 40,000 feet and correlated with reports of turbulence in the area. ^(7, 14) Another system was installed in a Boeing 727 jet and flown in areas of turbulence. A total of eight encounters with turbulence were recorded. The radar showed the presence of turbulence in each case. ⁽⁸⁾

Table 2 gives the parameters of the Boeing system, and Wallops Island (Atlas, et al).

Comparison of Table 2 with Table 1 indicates that the designed systems are not as good as the Wallops Island radar but better than the Boeing systems. The Wallops Island radar has detected a return from near the tropopause at a range of 12 Km. From these measurements, they calculated $C_n^2 = 4.4 \times 10^{-16} \text{ cm}^{-2/3}$, ⁽¹⁾ which lends support to the assumptions upon which the present system design is based. The Boeing ground system has detected disturbed refractive index at altitudes up to 38,000 feet with signal-to-noise ratios of 6 db or more. ⁽¹²⁾ The Boeing airborne radar has detected turbulence and encountered it with the airplane eight times during April and May 1966. The detection range is equal to the altitude of the airplane due to ground return, but signals from light turbulence (.3g vertical acceleration) were observed at ranges up to 30,000 feet ⁽⁸⁾.

Calculations and measurements with an M33 radar as reported in reference 23 show that the X-band radar will not detect turbulence. However, a few returns have been received that have not come from small targets but possibly from extended layers. ⁽²³⁾

The characteristics of this radar are

$$P_T = 250 \text{ Kw}$$

$$\tau = .25 \mu s$$

$$G_T = G_R = 40 \text{ db}$$

$$\text{Noise figure} = 13 \text{ db.}$$

Table 2

Existing Systems

	Boeing System		Wallops Island		
	ground	air			
	<u>Transmitter</u>				
λ	1.38 m	1.38 m	70 cm	10.7 cm	3.2 cm
P_T	120 Kw	200 Kw	7.5 Mw	4.5 Mw	170 Kw
PRF (pps)	60 to 200	60	960 or 320	320	320
τ	10 μ s	2-6 μ s	.1 to 6.2 μ s	2.2 μ s	1.8 μ s
P_{av}		50 w			
	<u>Receiver</u>				
NF	4 db	3.5 db			3.5 db
T_e		420°K	550°K	500°K	
Bw	200 kHz		.5 to 20 mHz	650 kHz	750 kHz
Antenna gain	22 db	18.3 db	35 db	51 db	56 db
Max. range for $C_n^2 = 10^{-16} \text{ cm}^{-2/3}$					
$\frac{S}{N} = 0 \text{ db}$	6.6 Km	3.9 Km	61.8 Km	75.7 Km	12.76 Km

VIII. CONCLUSIONS

This study of the radar parameters indicates that disturbed refractive index in the atmosphere may be detected by means of radar measurements with moderate power at short ranges. The most important features of the radar are antenna size and a receiver sensitivity. It is concluded that there is little difference in effectiveness of the system for wavelengths from 1 m to 10 cm as long as the same antenna size is used and the antenna beam is filled. For the purpose of analyzing the disturbed refractive index to determine what type of return signifies danger to airplanes, the smaller scattering volume obtained with wavelengths of 10 cm to 30 cm would probably give a more accurate estimate of the structure of the turbulent area as it passes through the antenna beam.

There are several practical difficulties which limit the usefulness of most present radar systems for turbulence detection. The most serious of these is minimum range performance. Recovery time and clutter level usually restrict most radar systems to a relatively long range at which the turbulent scattering signal is lost in the noise.

Therefore, even though little success has been attained with conventional radar in detecting turbulent regions in the atmosphere, a specially designed research system should have little trouble in the detection and analysis of the signal from regions of disturbed refractive index of the atmosphere at lower elevation.

The optimum wavelength will lie somewhere around 10 cm to 30 cm. This choice is due to the wavelength dependence of the scattering cross section and the limits on antenna size and gain.

The antenna will have a maximum diameter of 15 meters and a maximum gain of 50 db. At wavelengths shorter than 11 cm, the size is limited by the gain consideration.

In order to use moderate transmitter power (about one to three megawatts peak), the receiver will need to have a low noise preamplifier. From these studies, it is concluded that a radar for airborne detection of disturbed refractive index has severe practical limitations. The most important limitations are antenna size and transmitter power.

BIBLIOGRAPHY

1. Atlas, D. A., Hardy, K. R., and Glover, K. M., "Tropopause Detected by Radar," Science, Vol. 153, Sept. 1966.
2. Atlas, D., Hardy, K. R. and Naito, K., "Optimizing the Radar Detection of Clear Air Turbulence," paper presented at National Air Meeting on Clear Air Turbulence, Washington, D. C., Feb. 23-24, 1966.
3. Barton, D. K., Radar System Analysis, Prentice-Hall, Inc., Englewood Cliffs, New Jersey, 1965.
4. Berkowitz, R.S. (Editor), Modern Radar, John Wiley and Sons, Inc. New York, 1965.
5. Bickmore, R.W., and Hansen, R.C., "Antenna Power Densities in the Fresnel Region," Proc. IRE, Vol. 47, Dec. 1959.
6. Buehler, W.E., and Lunden, C.D., "Radar Detection of Turbulence in the Upper Troposphere," Document No. D6-17489, Boeing Airplane Co., Transport Div., Renton, Washington, 1964.
7. Buehler, W. E., and Lunden, C.D., "A note on VHF Backscatter from Turbulence in the Upper Troposphere," Journal of Applied Meteorology, Vol. 4, No. 1, Feb. 1965.
8. Buehler, W.E., and Lunden, C.D., "Airborne CAT Detection by VHF Radar," Document No. D6-15528, Boeing Co., Airplane Div., Renton, Washington, 1967.

9. Deam, A. P. and Walker, G. B., "High Altitude Microvariations Within the Atmosphere's Radio Refractive Index Profile," The University of Texas, EERL Report No. 6-52, February 1963.
10. Fannin, B. M., "Remote Detection of Clear Air Turbulence: Part I - Pulsed Microwave Radars," The University of Texas, EERL Report No. P-13, November 1966.
11. Fusca, J. A., "Clear Air Turbulence," Space/Aeronautics, August 1964.
12. King, C. H. and Buehler, W. E., "A VHF Radar for the Detection of Atmospheric Turbulence," Document No. D6-17489, Boeing Airplane Co., Transport Div., Renton, Washington, 1964.
13. LaGrone, A. H., Deam, A. P., and Walker, G. B., "Angels, Insects, and Weather," Radio Science, Journal of Research, Vol. 68D, No. 8, August 1964.
14. Lunden, C. D., "Clear Air Turbulence Radar Studies," Document No. D6-17722, Boeing Airplane Co., Transport Div., Renton, Washington, 1965.
15. Probert-Jones, J. R., "The Radar Equation in Meteorology," Quart. Journal of Royal Meteorological Society, No. 88, 1962.
16. Reiter, E. R., Jet-stream Meteorology, University of Chicago Press, 1963.
17. Saxton, J. A., Lane, J. A., Meadows, R. W., and Matthews, P. A., "Layer Structure of the Troposphere," Proc. IEE, Vol. 111, Feb. 1964.

18. Saxton, J. A., (Editor), Advances in Radio Research, Academic Press, New York, 1964.
19. Schwartz, M., Information Transmission, Modulation and Noise, McGraw-Hill Book Company, Inc., New York, 1959.
20. Silver, S. (Editor), Microwave Antenna Theory and Design, M. I. T. Radiation Laboratory Series, Vol. 12, McGraw-Hill Book Co., Inc., New York, 1949.
21. Skolnik, M. I., Introduction to Radar Systems, McGraw-Hill Book Co., Inc., New York, 1962.
22. Smith, P. L., and Rogers, R. R., "On the Possibility of Radar Detection of Clear Air Turbulence," 10th Weather Radar Conference, Washington, D. C., 1963.
23. Stephens, J. J., "Note on the Idealized Radar Range Equation," The University of Texas, EERL Report No. P-5, May 1966.
24. Stephens, J. J., and Reiter, E. R., "Estimating Refractive Index Spectra in Regions of Clear Air Turbulence," The University of Texas, EERL Report No. P-12, October 1966.
25. Tatarski, V. I., Wave Propagation in a Turbulent Medium, McGraw-Hill Book Co., Inc., New York, 1961.
26. Westman, H. P. (Editor), Reference Data for Radio Engineers, International Telephone and Telegraph Corp., New York, 1956.